Electronic Supplementary Information

Application of roof shape amines as chiral solvating agents for discrimination of optically active acids by NMR spectroscopy: Study of match-mismatch effect and crystal structure of the diastereomeric salts

Riddhi Gupta,[a] Rajesh G. Gonnade[b] and Ashutosh V. Bedekar[a,]*

[a]Department of Chemistry, Faculty of Science, M. S. University of Baroda, Vadodara 390 002, India

[b]Center for Materials Characterization, CSIR-National Chemical Laboratory, Dr. Homi Bhabha Road, Pune 411 008, India

Tel. No. +91(265)2795552; Email: avbedekar@yahoo.co.in

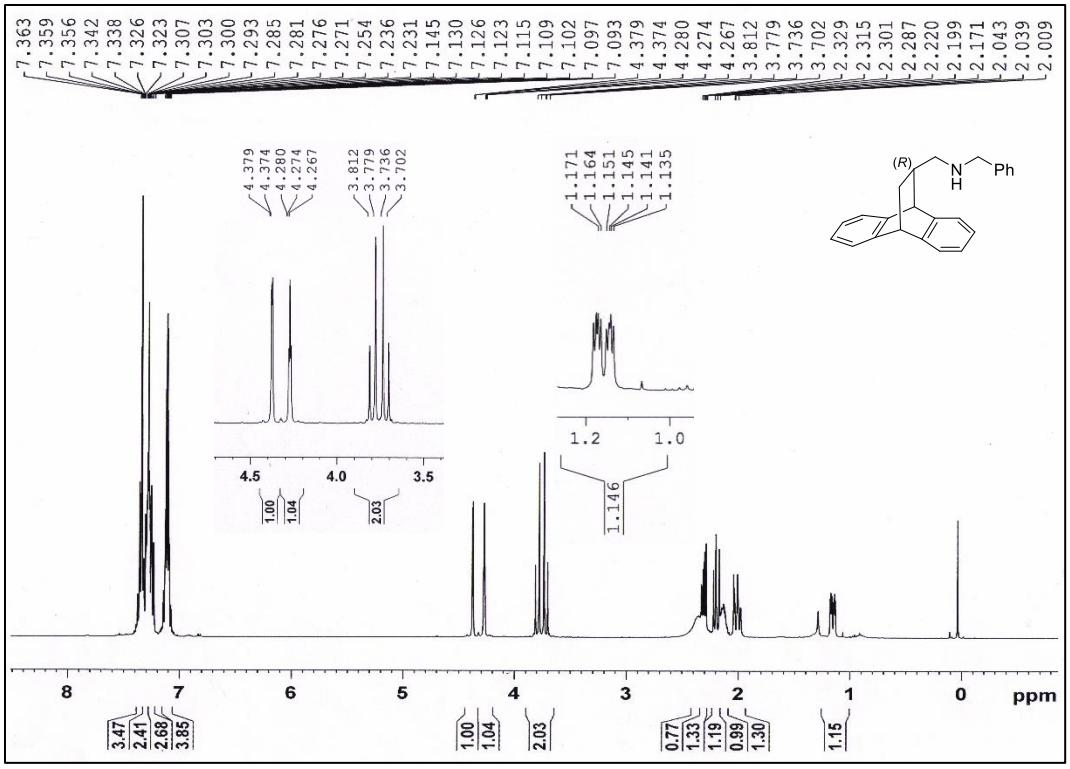

Figure 1: ^{1}H NMR Spectra of *(R)*-**2** ($CDCl_3$, 400MHz)

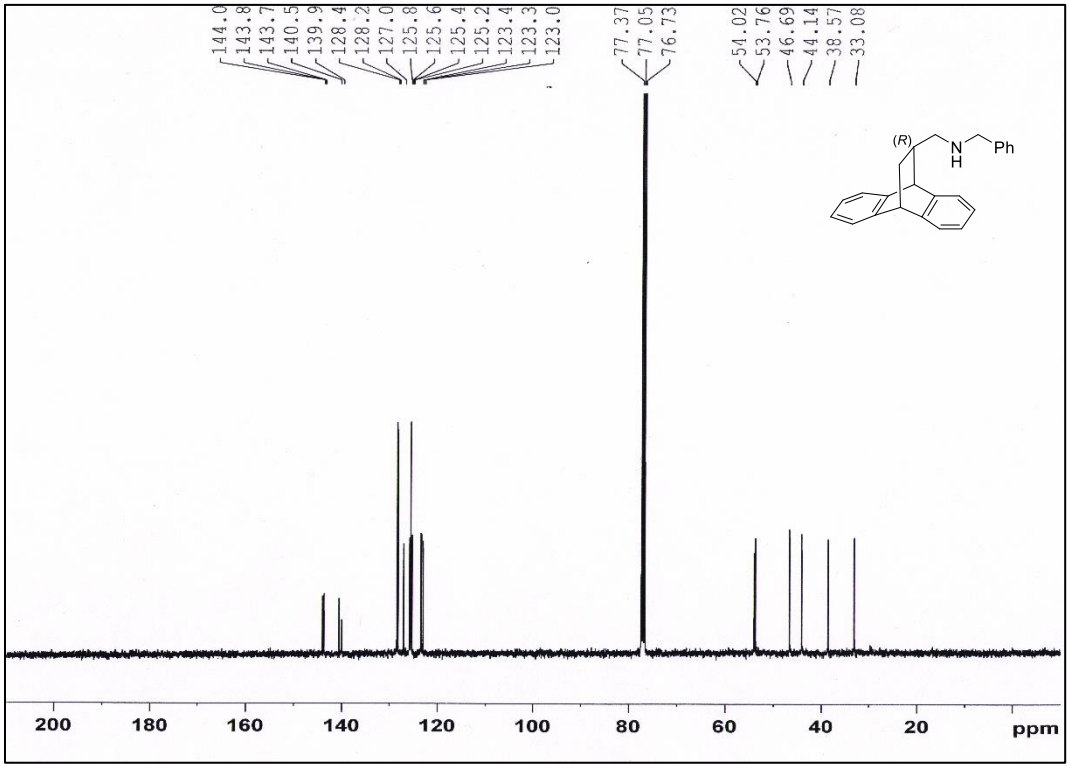

Figure 2: ^{13}C NMR Spectra of *(R)*-**2** ($CDCl_3$, 100MHz)

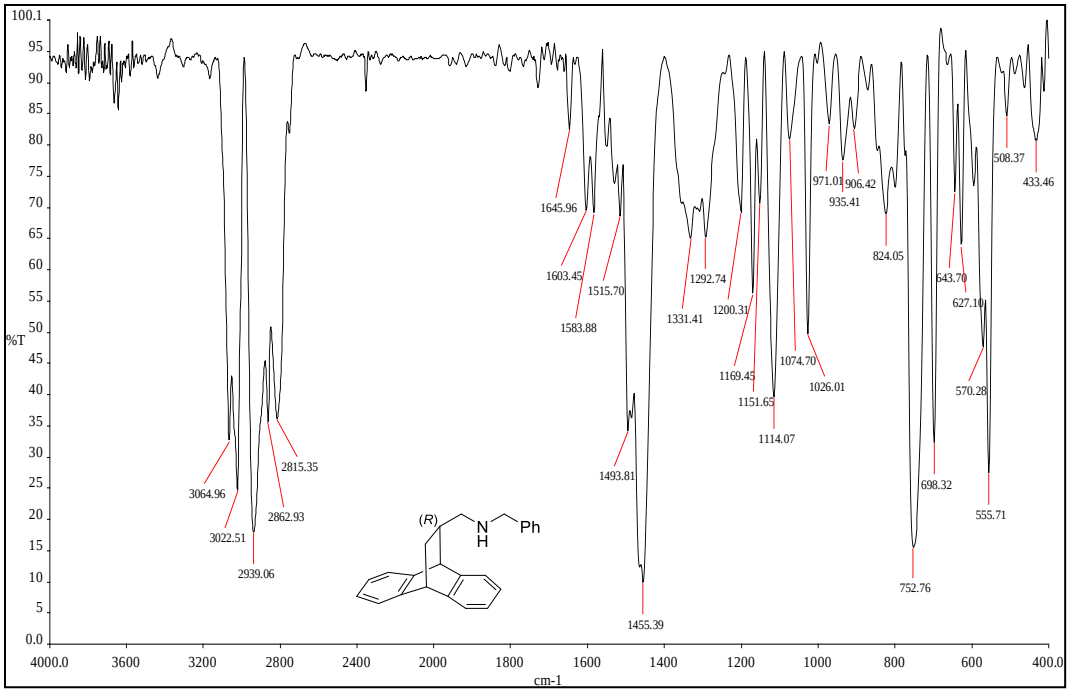

Figure 3: IR Spectra of *(R)*-**2**

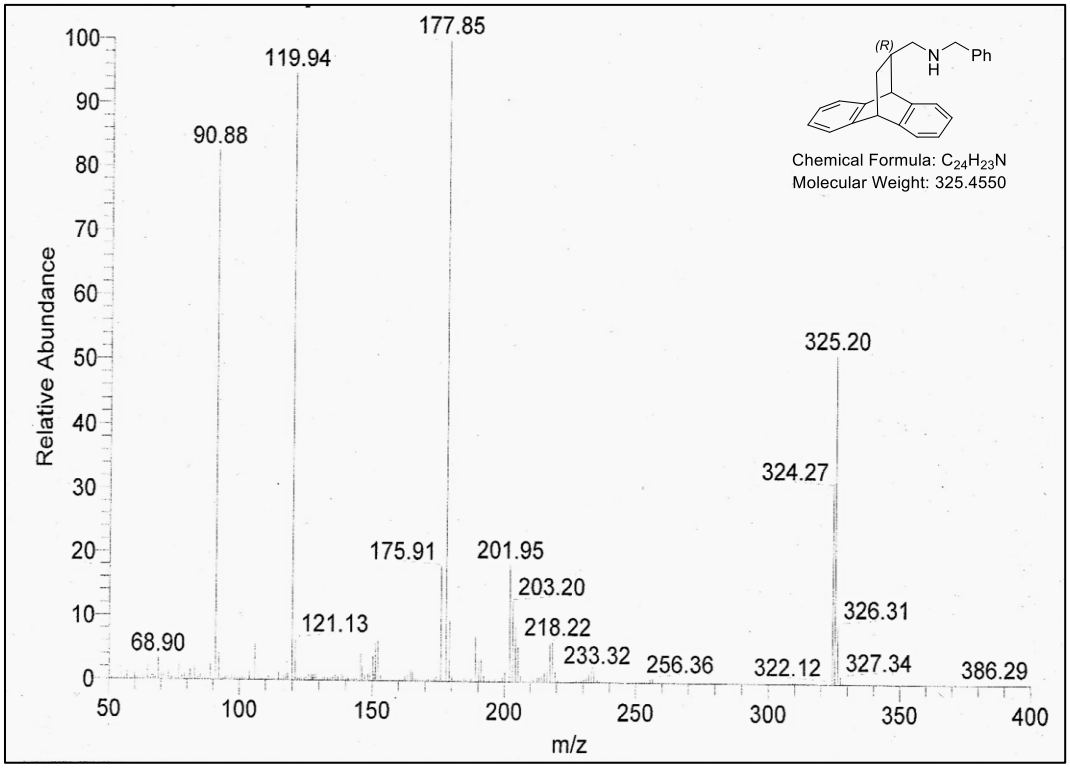

Figure 4: Mass Spectra of *(R)*-**2**

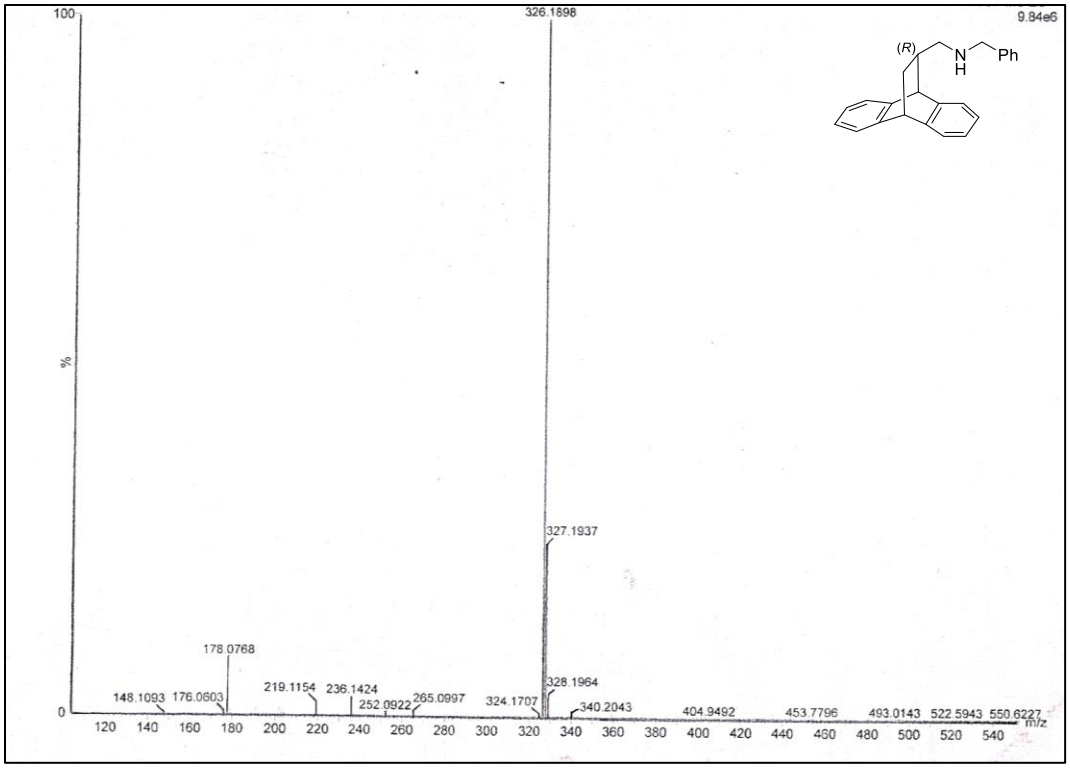

Figure 5: HRMS Spectra of *(R)*-**2**

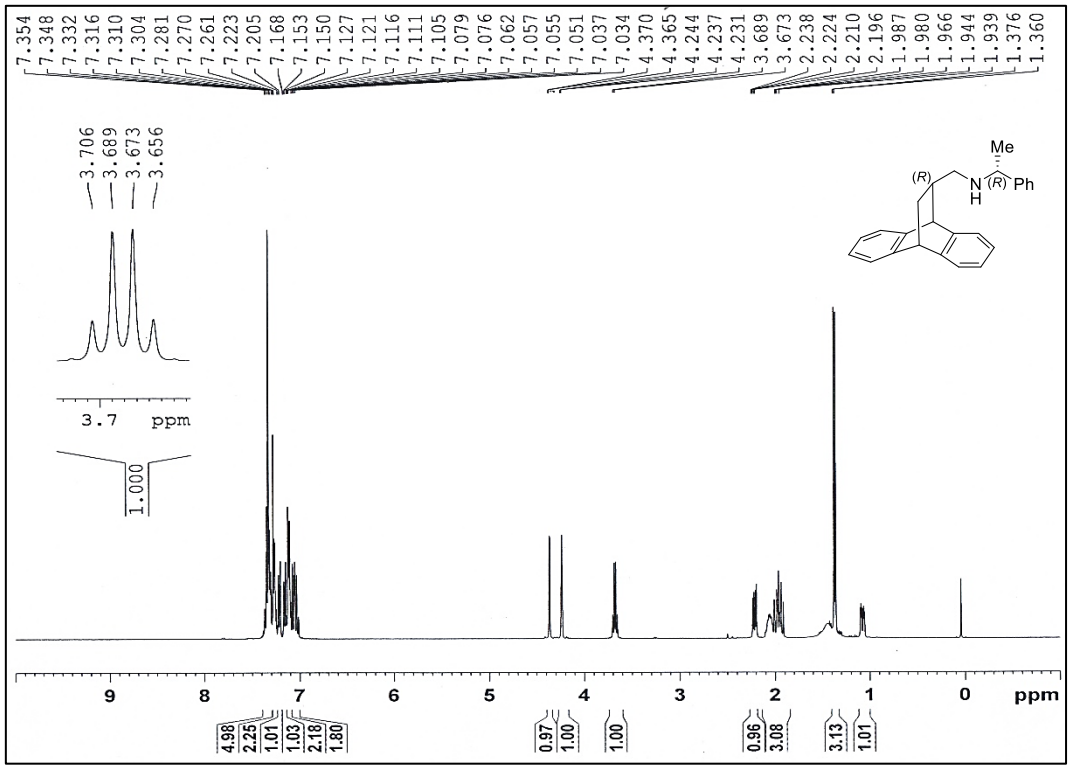

Figure 6: ^{1}H NMR Spectra of *(R,R)*-**3** ($CDCl_3$, 400MHz)

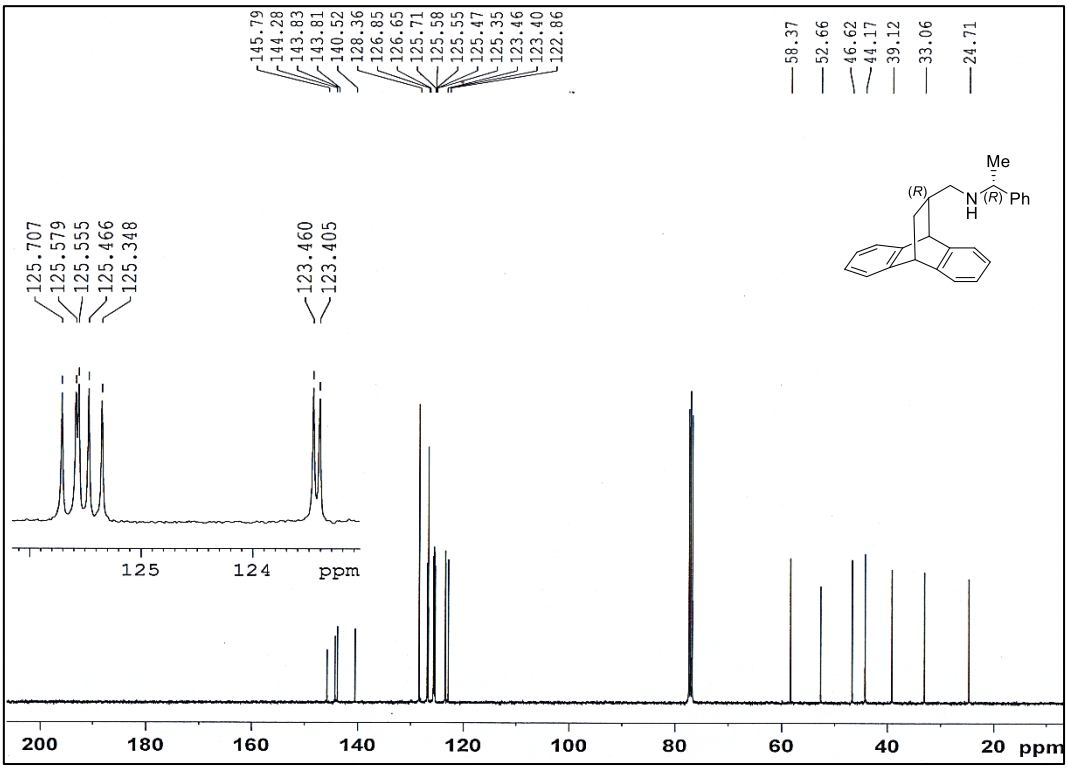

Figure 7: ^{13}C NMR Spectra of *(R,R)*-**3** ($CDCl_3$, 100MHz)

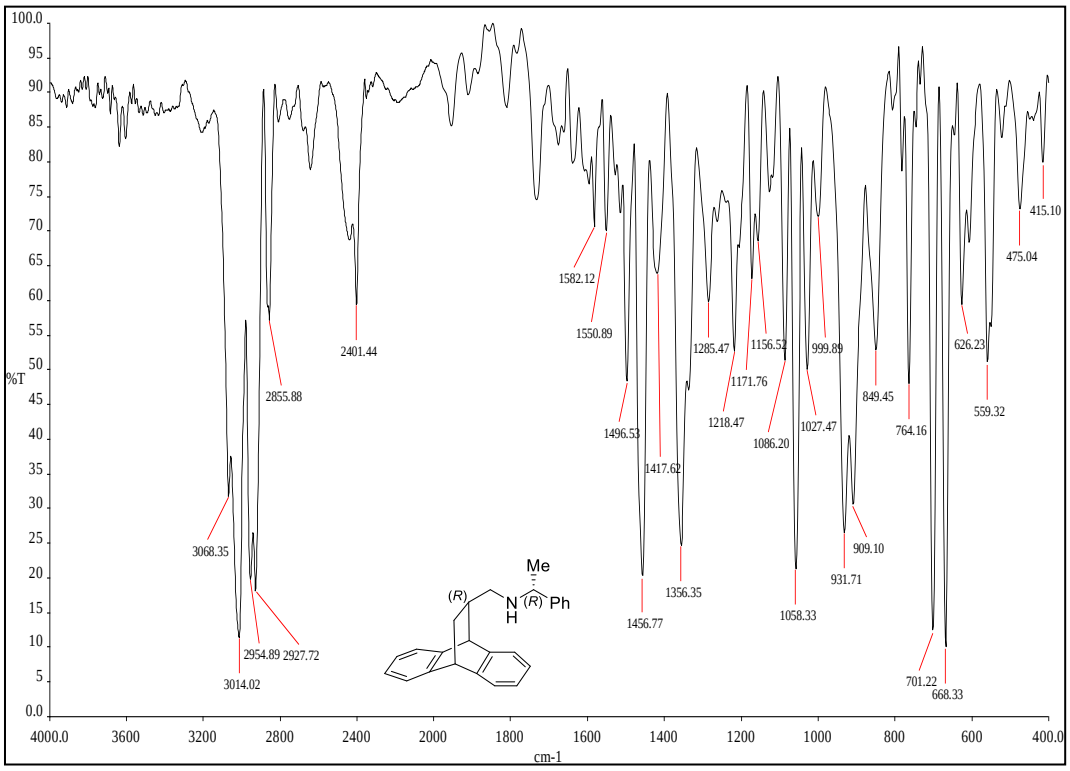

Figure 8: IR Spectra of *(R,R)*-**3**

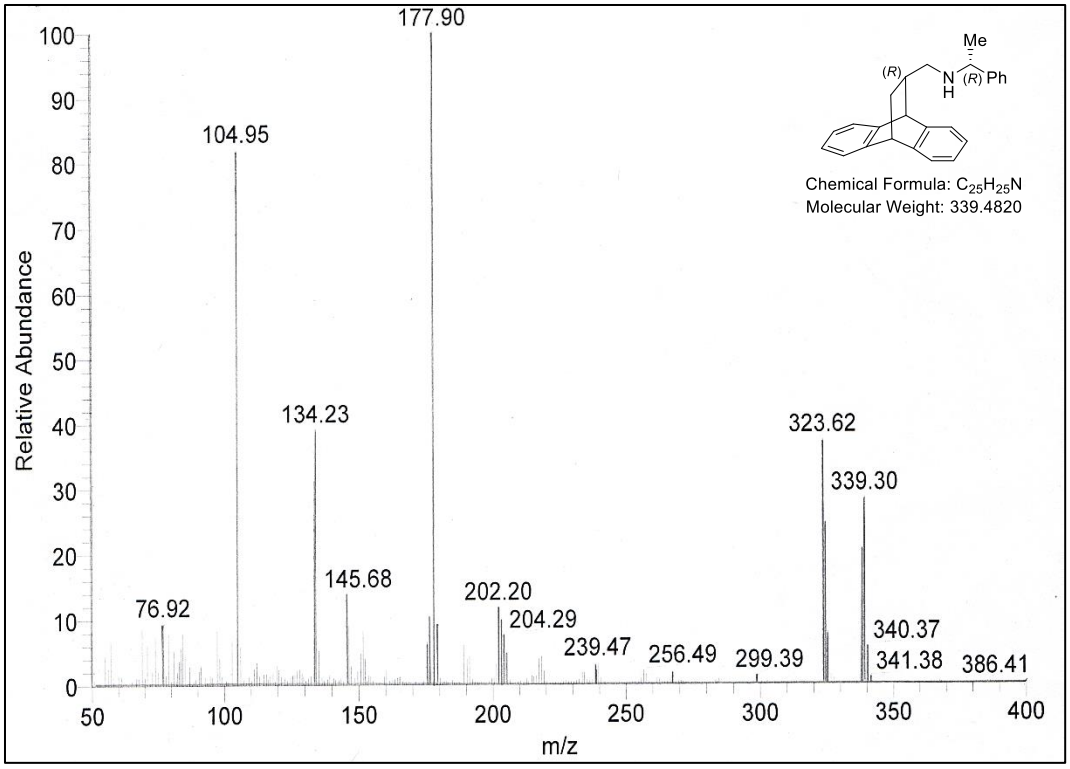

Figure 9: Mass Spectra of *(R,R)*-**3**

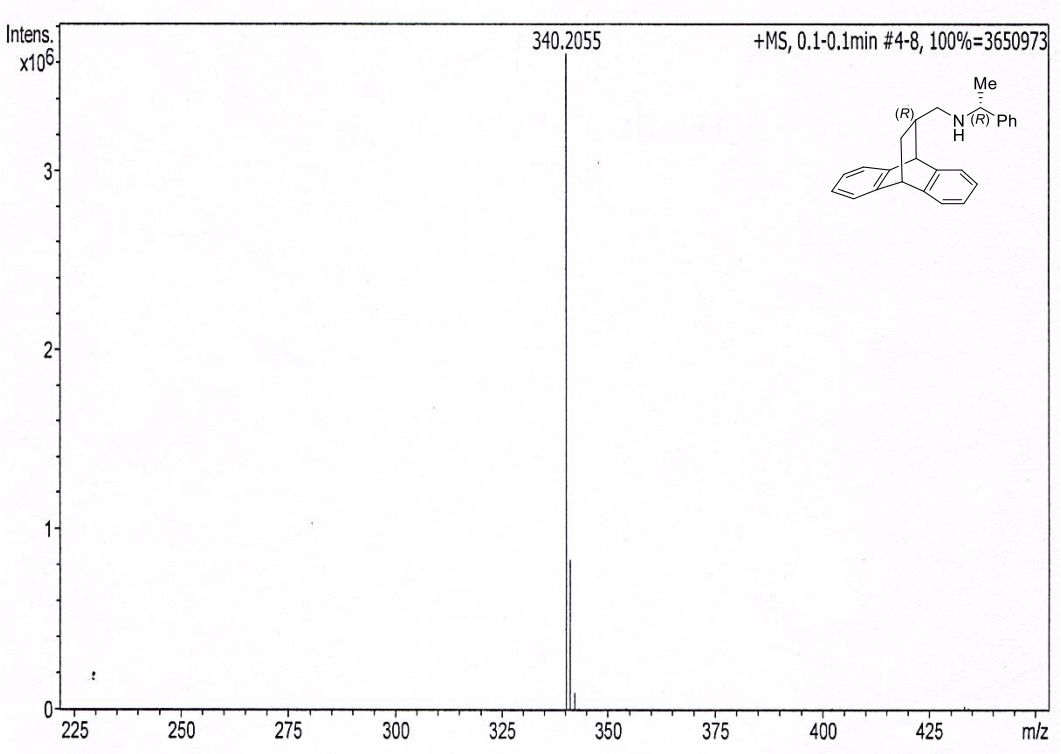

Figure 10: HRMS Spectra of *(R,R)*-**3**

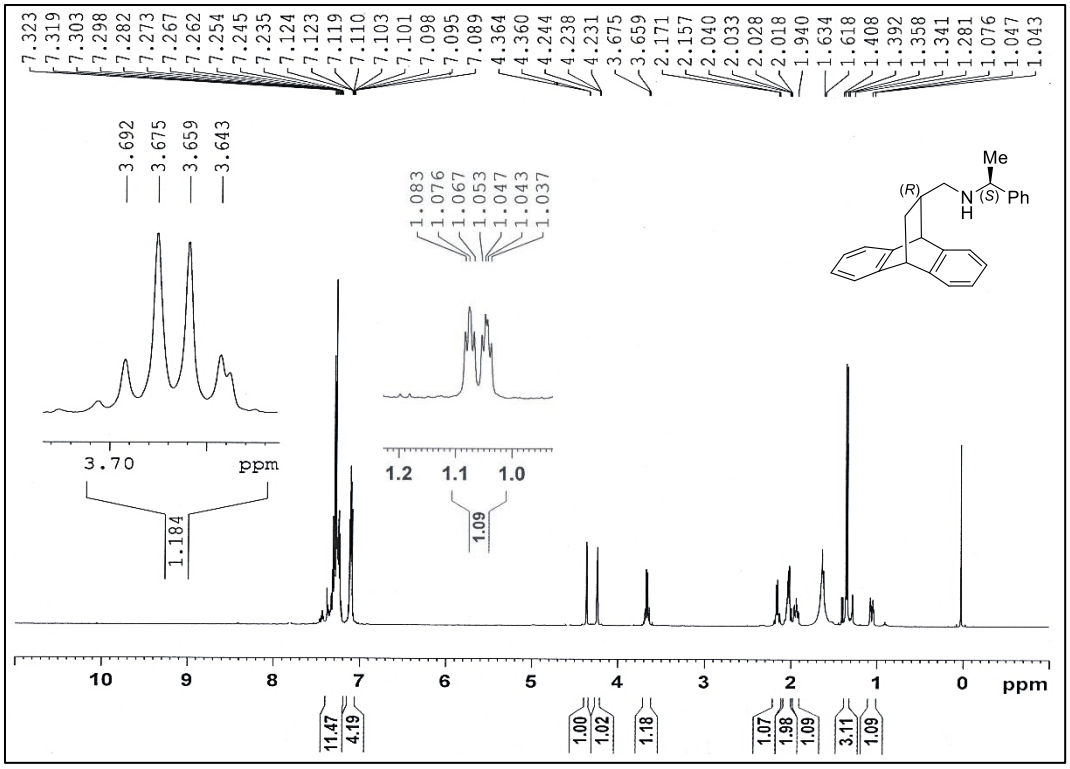

Figure 11: ^{1}H NMR Spectra of *(R,S)*-**3** ($CDCl_3$, 400MHz)

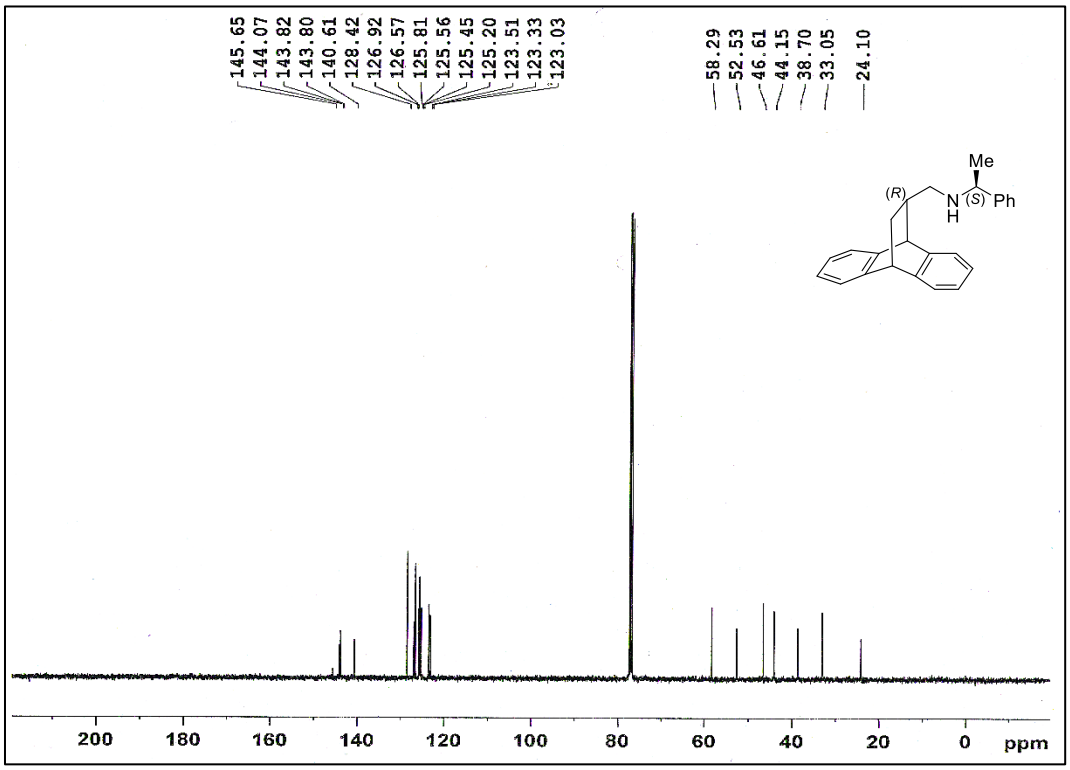

Figure 12: ^{13}C NMR Spectra of *(R,S)*-**3** ($CDCl_3$, 100MHz)

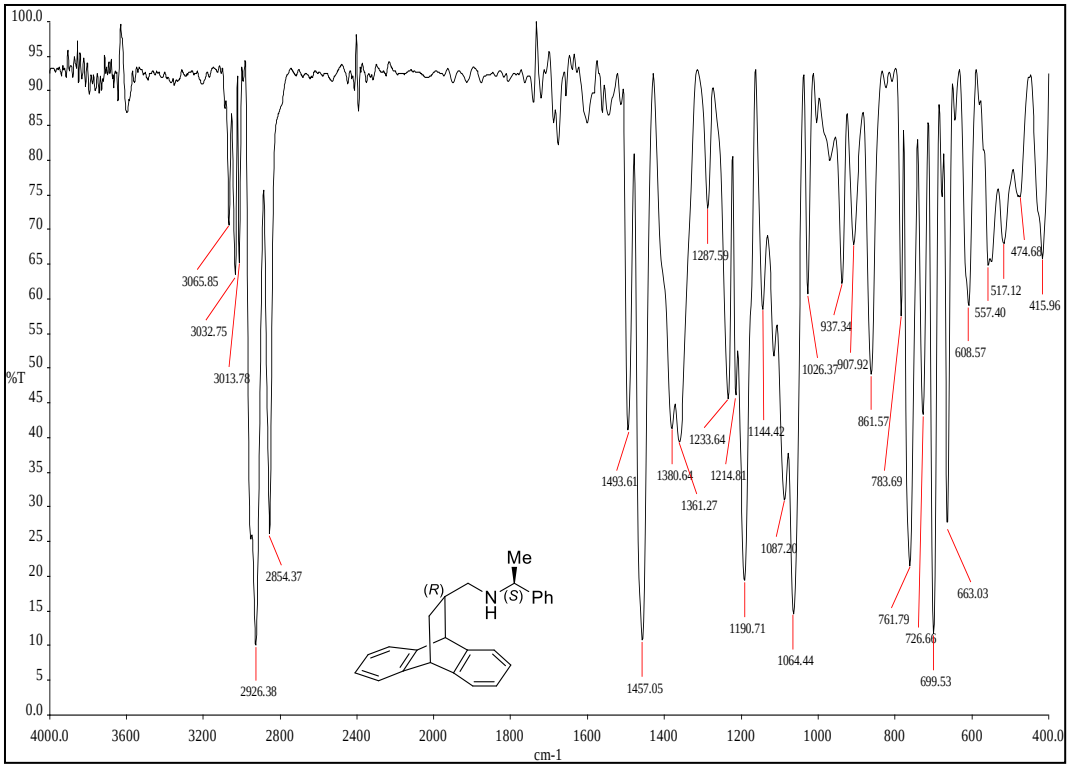

Figure 13: IR Spectra of *(R,S)*-**3**

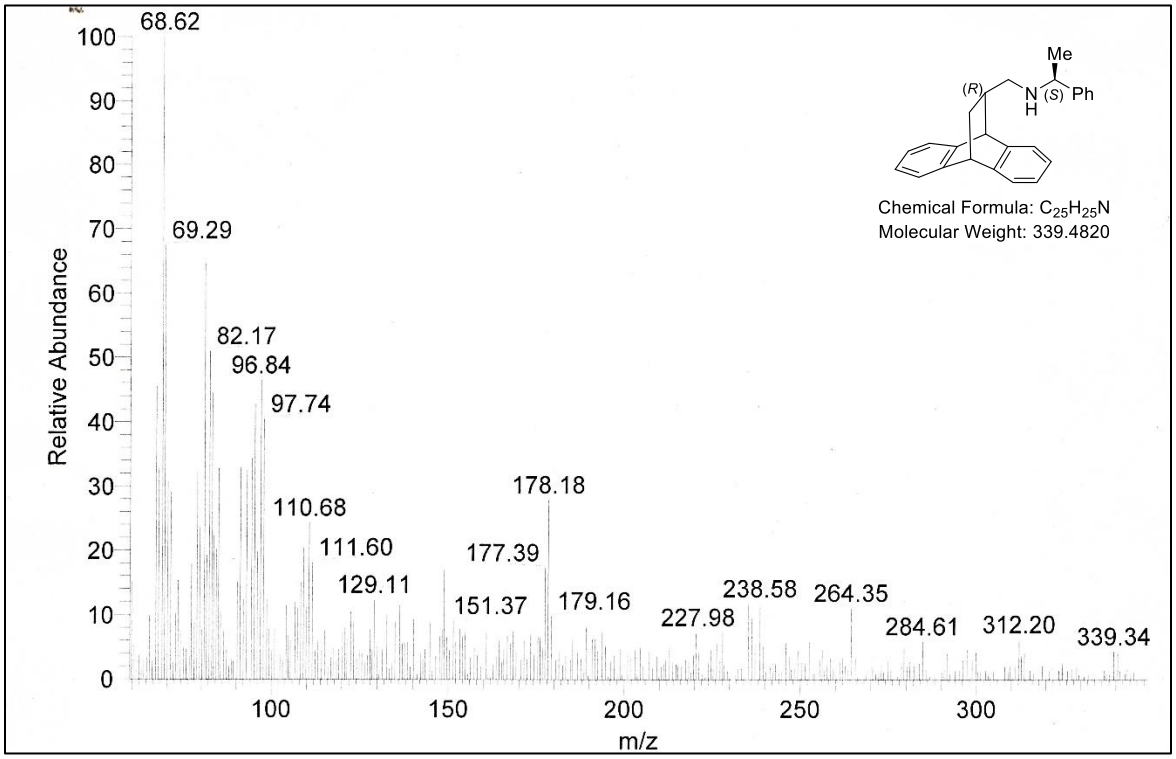

Figure 14: Mass Spectra of *(R,S)*-**3**

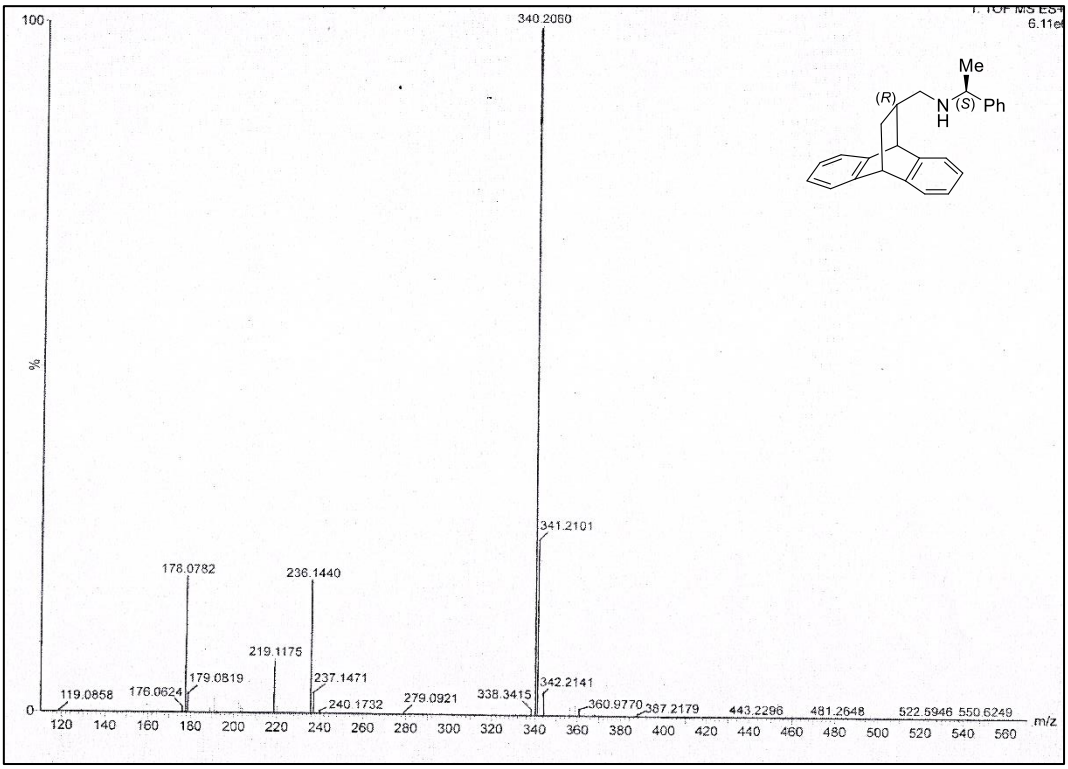

Figure 15: HRMS Spectra of *(R,S)*-**3**

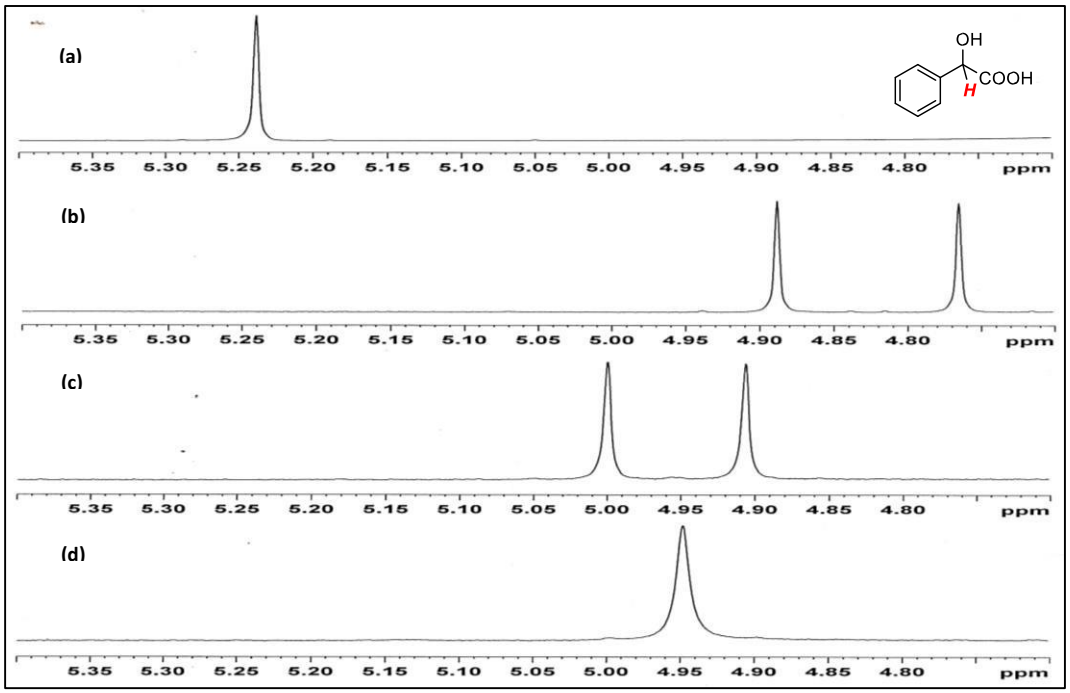

Figure 16: ^{1}H NMR Spectra of: (a) (±) Mandelic acid (b) (±) Mandelic acid & *(R)*-**2** (c) (±) Mandelic acid & *(R,R)*-**3** (d) (±) Mandelic acid & *(R,S)*-**3**

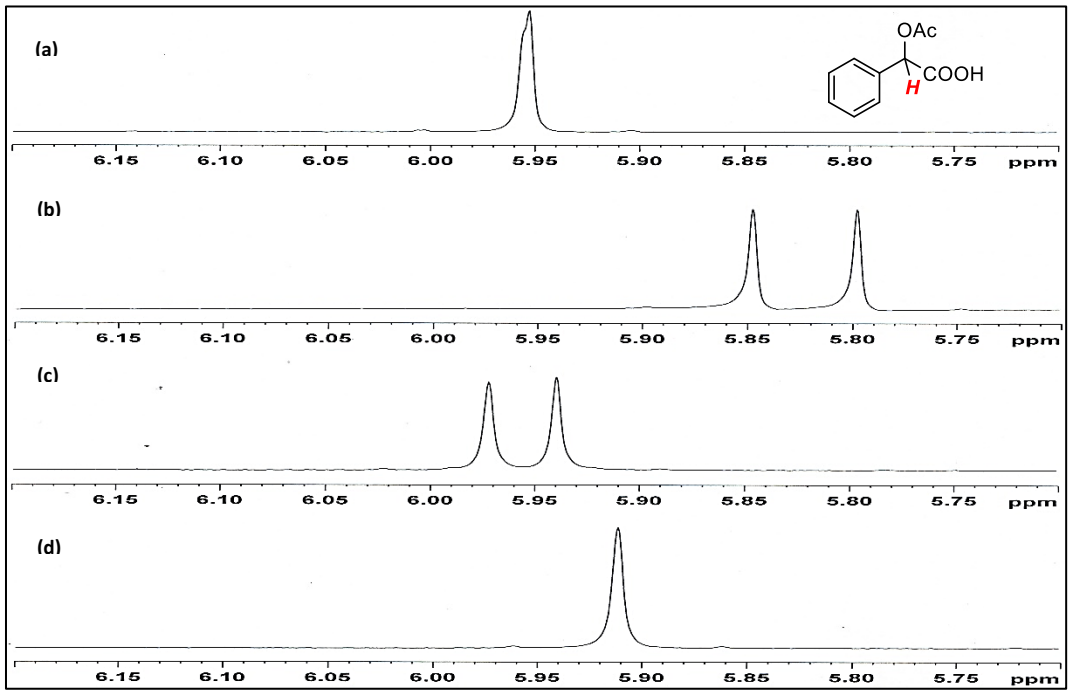

Figure 17: ^{1}H NMR Spectra of: (a) (±) O-AcetylMandelic acid (b) (±) O-AcetylMandelic acid & *(R)*-**2** (c) (±) O-AcetylMandelic acid & *(R,R)*-**3** (d) (±) O-AcetylMandelic acid & *(R,S)*-**3**

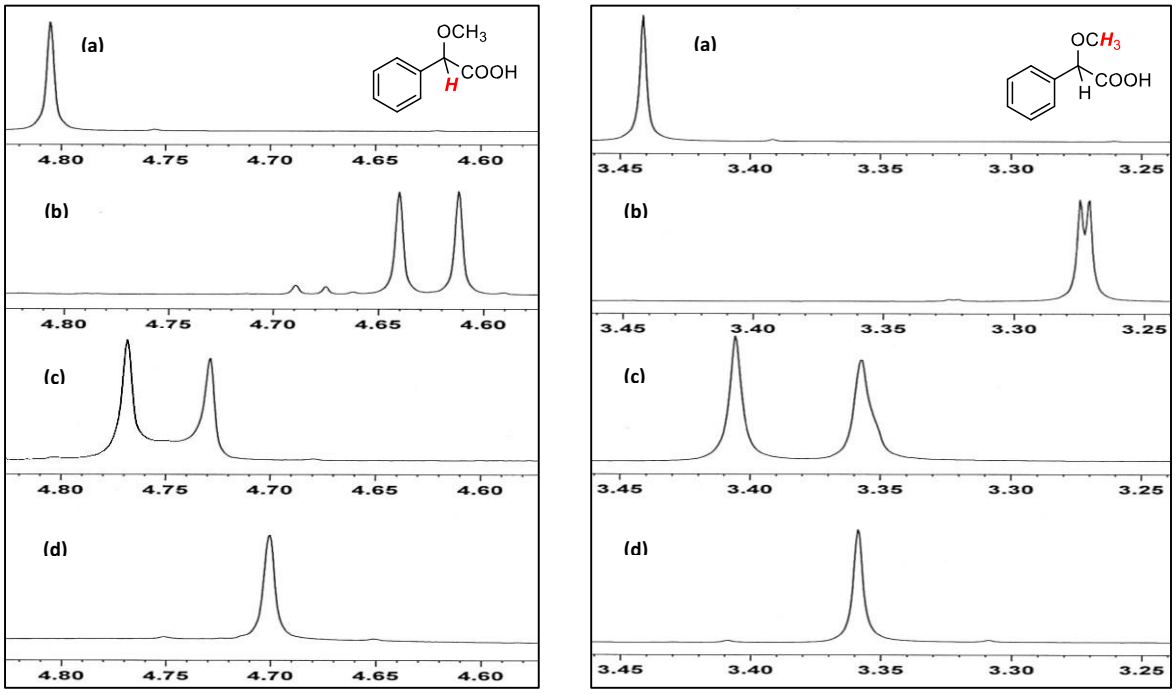

Figure 18: ^{1}H NMR Spectra of: (a) (±) O-Methylmandelic acid (b) (±) O-Methylmandelic acid & *(R)*-**2** (c) (±) O-Methylmandelic acid & *(R,R)*-**3** (d) (±) O-Methylmandelic acid & *(R,S)*-**3**

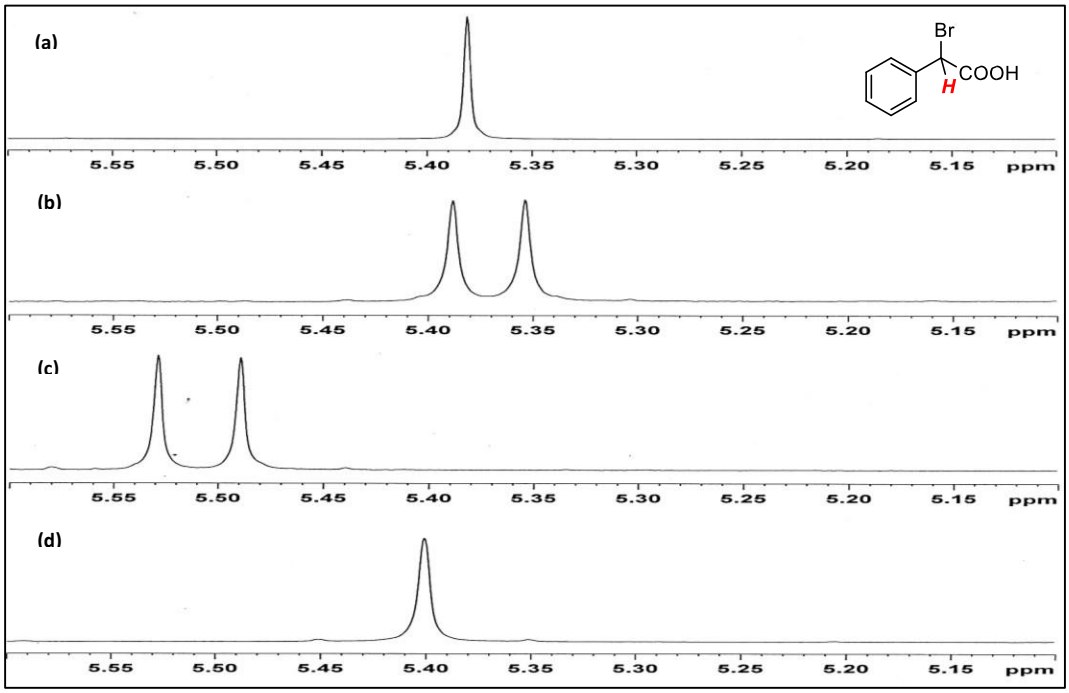

Figure 19: ^{1}H NMR Spectra of: (a) (±)α-Bromo phenylacetic acid (b) (±)α-Bromo phenylacetic acid & *(R)*-**2** (c) (±) α-Bromo phenylacetic acid & *(R,R)*-**3** (d) (±)α-Bromo phenylacetic acid & *(R,S)*-**3**

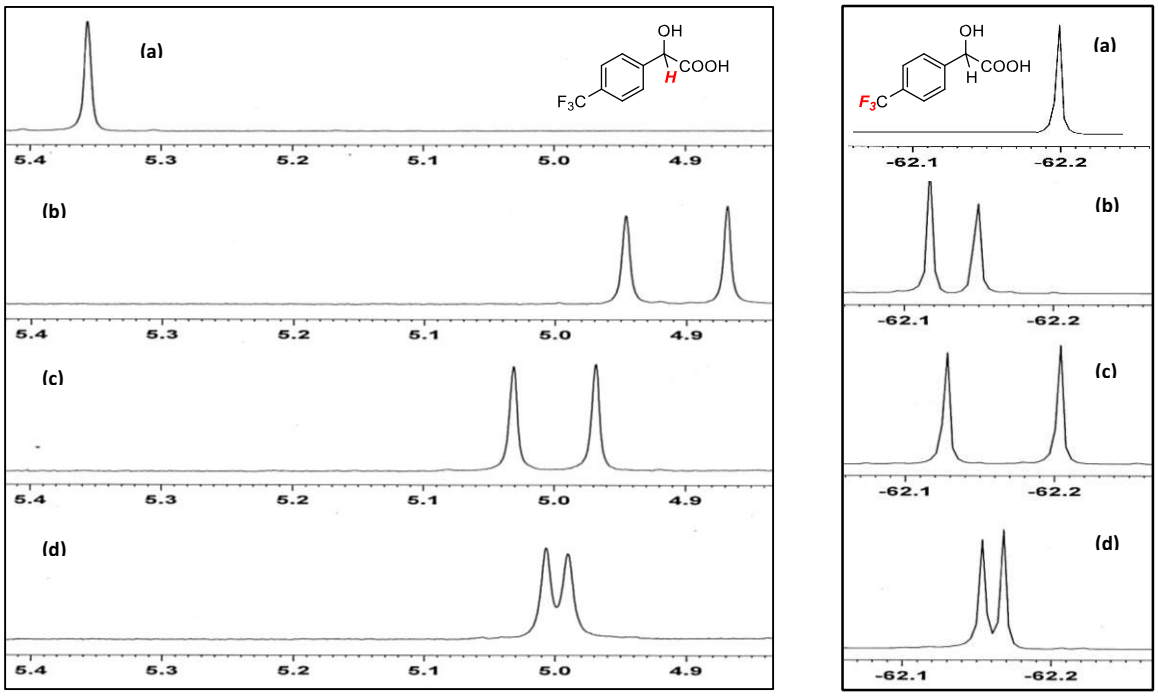

Figure 20: ^{1}H & ^{19}F NMR Spectra of: (a) (±) 4-Trifluoromethylmandelic acid (b) (±) 4-Trifluoromethylmandelic acid & *(R)*-**2** (c) (±) 4-Trifluoromethylmandelic acid & *(R,R)*-**3** (d) (±) 4-Trifluoromethylmandelic acid & *(R,S)*-**3**

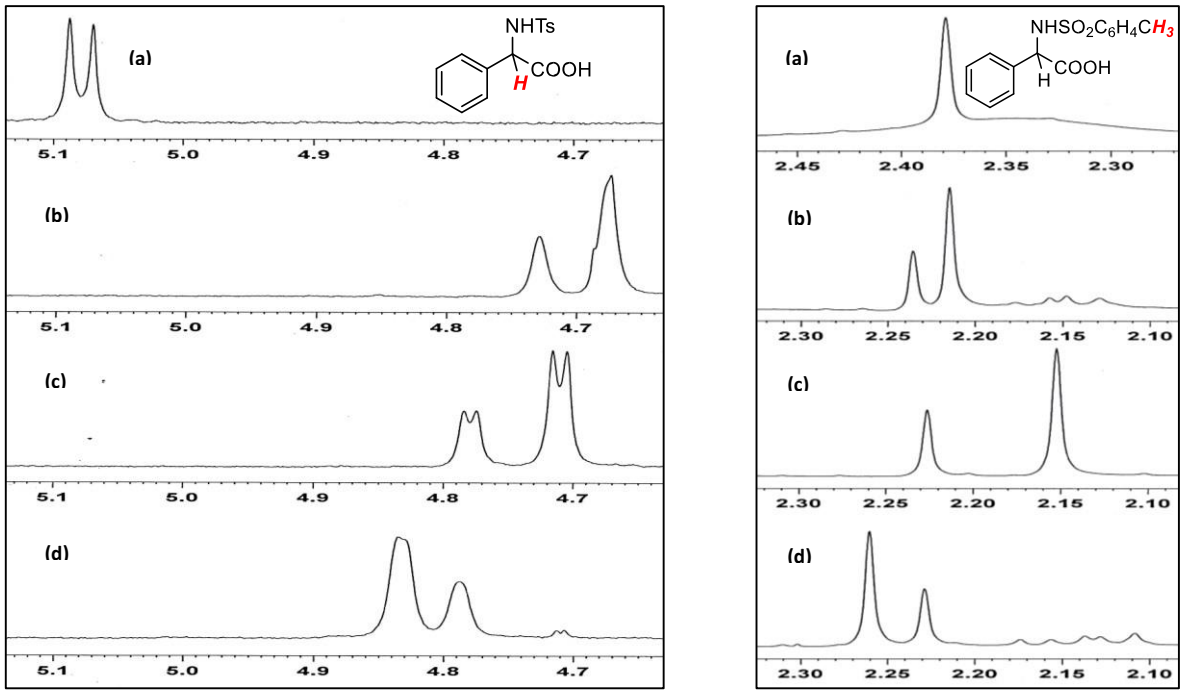

Figure 21: ^{1}H NMR Spectra of: (a) N-Tosylphenyl glycine(*R*:*S* 65:35) (b) N-Tosylphenyl glycine(*R*:*S* 65:35) & *(R)*-**2** (c) N-Tosylphenyl glycine(*R*:*S* 65:35) & *(R,R)*-**3** (d) N-Tosylphenyl glycine(*R*:*S* 65:35) & *(R,S)*-**3**

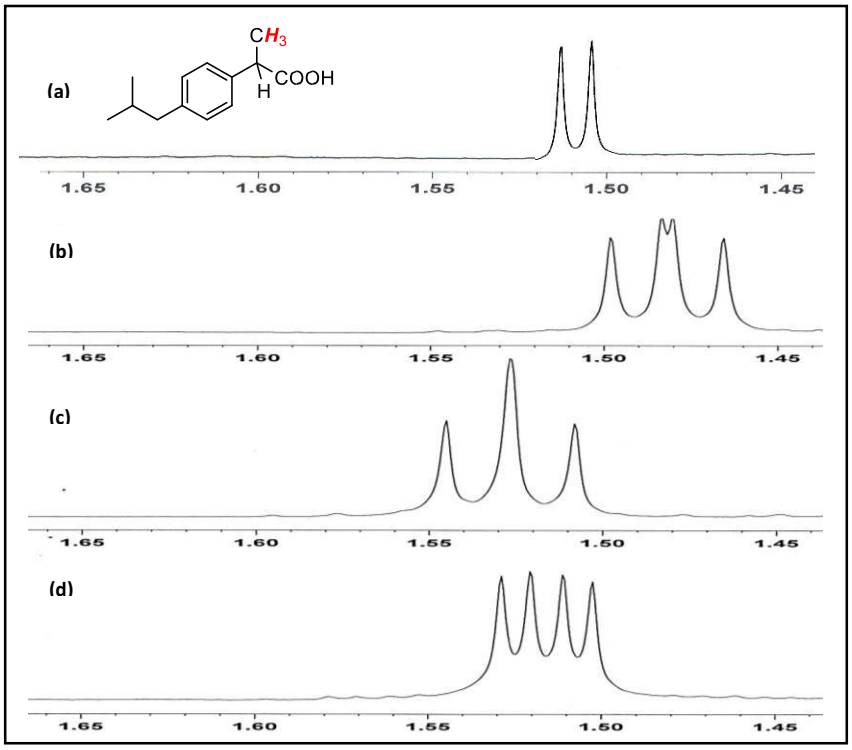

Figure 22: ^{1}H NMR Spectra of: (a) (±) ibuprofen (b) (±) ibuprofen & *(R)*-**2** (c) (±) ibuprofen & *(R,R)*-**3** (d) (±) ibuprofen & *(R,S)*-**3**

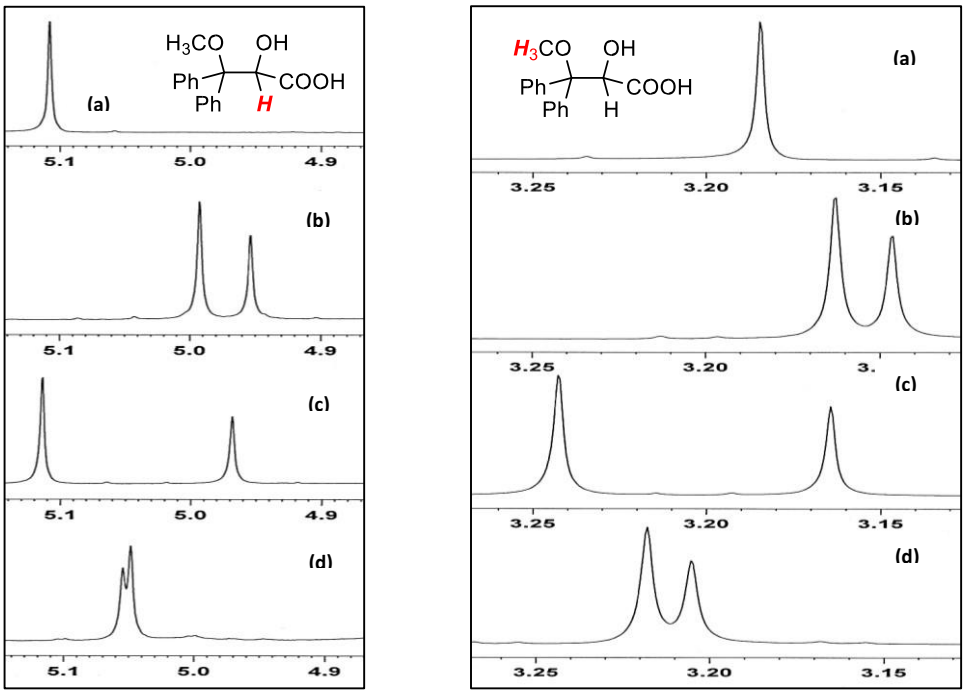

Figure 23: ^{1}H NMR Spectra of: (a) 2-hydroxy-3-methoxy-3,3-diphenyl propanoic acid (*S*:*R* 60:40) (b) 2-hydroxy-3-methoxy-3,3-diphenyl propanoic acid (*S*:*R* 60:40) & *(R)*-**2** (c) 2-hydroxy-3-methoxy-3,3-diphenyl propanoic acid (*S*:*R* 60:40) & *(R,R)*-**3** (d) 2-hydroxy-3-methoxy-3,3-diphenyl propanoic acid (*S*:*R* 60:40) & *(R,S)*-**3**

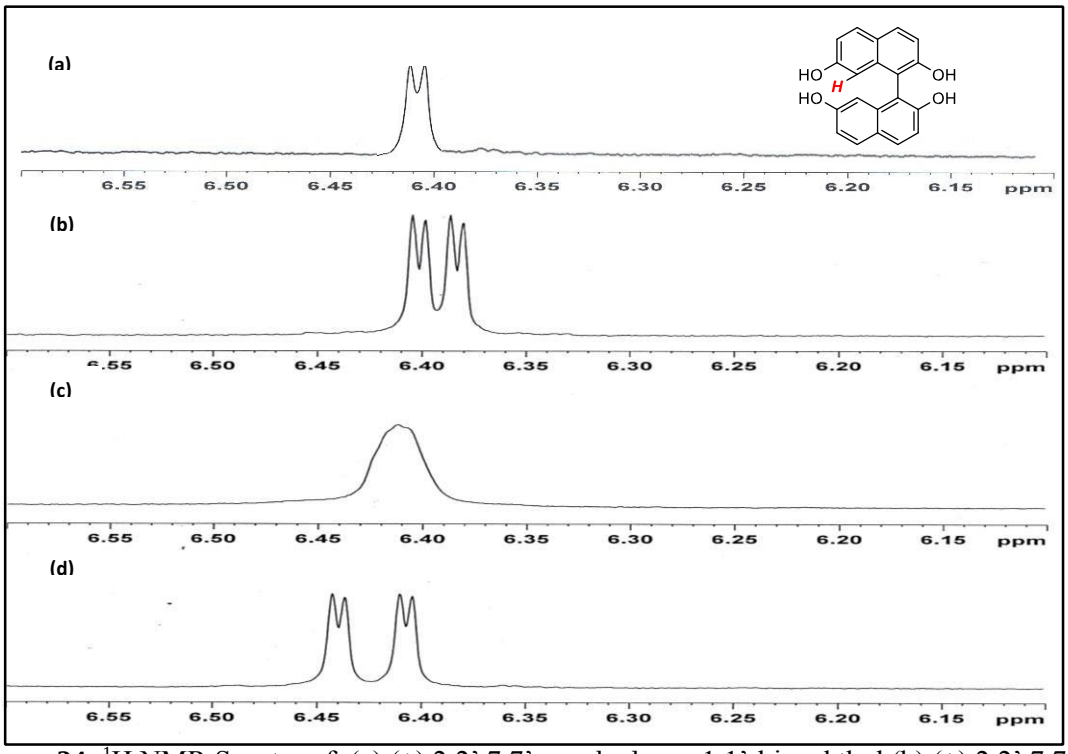

Figure 24: [1]H NMR Spectra of: (a) (±) 2,2',7,7'-tetrahydroxy-1,1'-binaphthyl (b) (±) 2,2',7,7'-tetrahydroxy-1,1'-binaphthyl & *(R)*-**2** (c) (±) 2,2',7,7'-tetrahydroxy-1,1'-binaphthyl & *(R,R)*-**3** (d) (±) 2,2',7,7'-tetrahydroxy-1,1'-binaphthyl & *(R,S)*-**3**

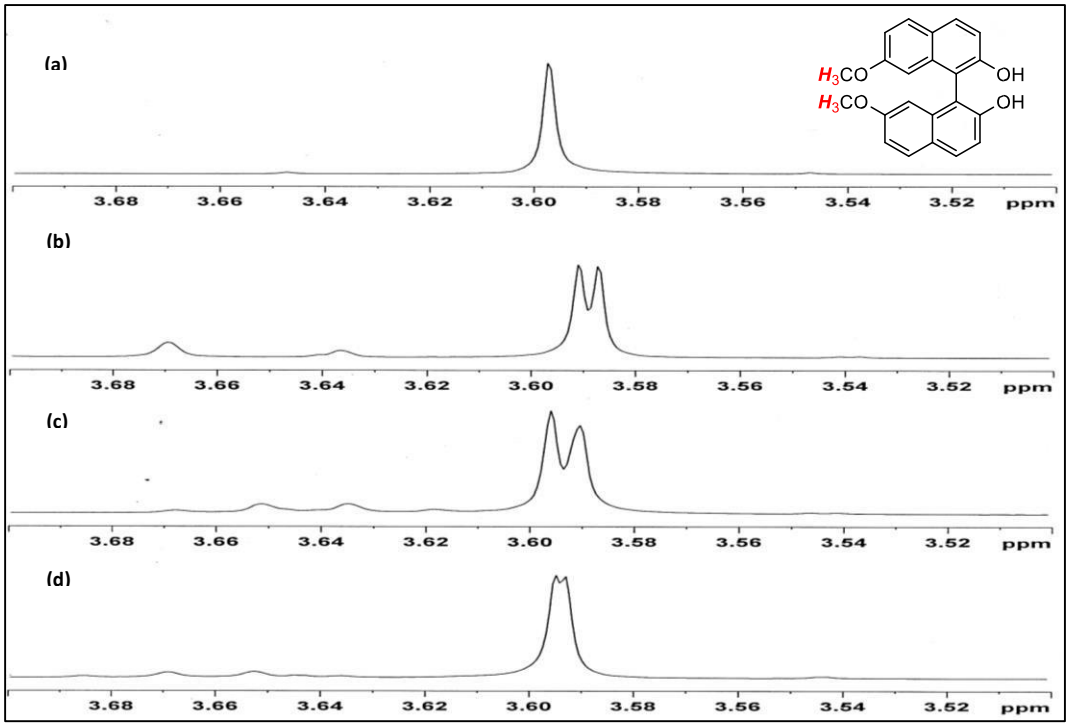

Figure 25: [1]H NMR Spectra of: (a) (±) 7,7'-dimethoxy-2,2'-dihydroxy-1,1'-binaphthyl (b) (±) 7,7'-dimethoxy-2,2'-dihydroxy-1,1'-binaphthyl & *(R)*-**2** (c) (±) 7,7'-dimethoxy-2,2'-dihydroxy-1,1'-binaphthyl & *(R,R)*-**3** (d) (±)7,7'-dimethoxy-2,2'-dihydroxy-1,1'-binaphthyl & *(R,S)*-**3**

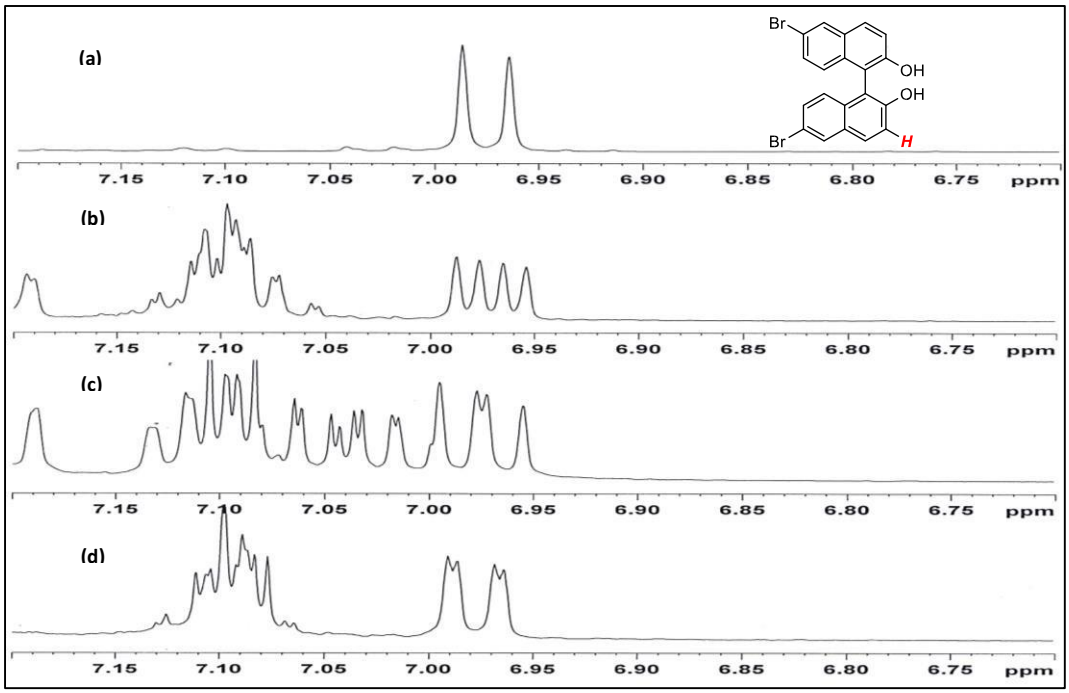

Figure 26: ^{1}H NMR Spectra of: (a) (±) 6,6'-dibromo-2,2'-dihydroxy-1,1'-binaphthyl (b) (±) 6,6'-dibromo-2,2'-dihydroxy-1,1'-binaphthyl & *(R)*-**2** (c) (±) 6,6'-dibromo-2,2'-dihydroxy-1,1'-binaphthyl & *(R,R)*-**3** (d) (±) 6,6'-dibromo-2,2'-dihydroxy-1,1'-binaphthyl & *(R,S)*-**3**

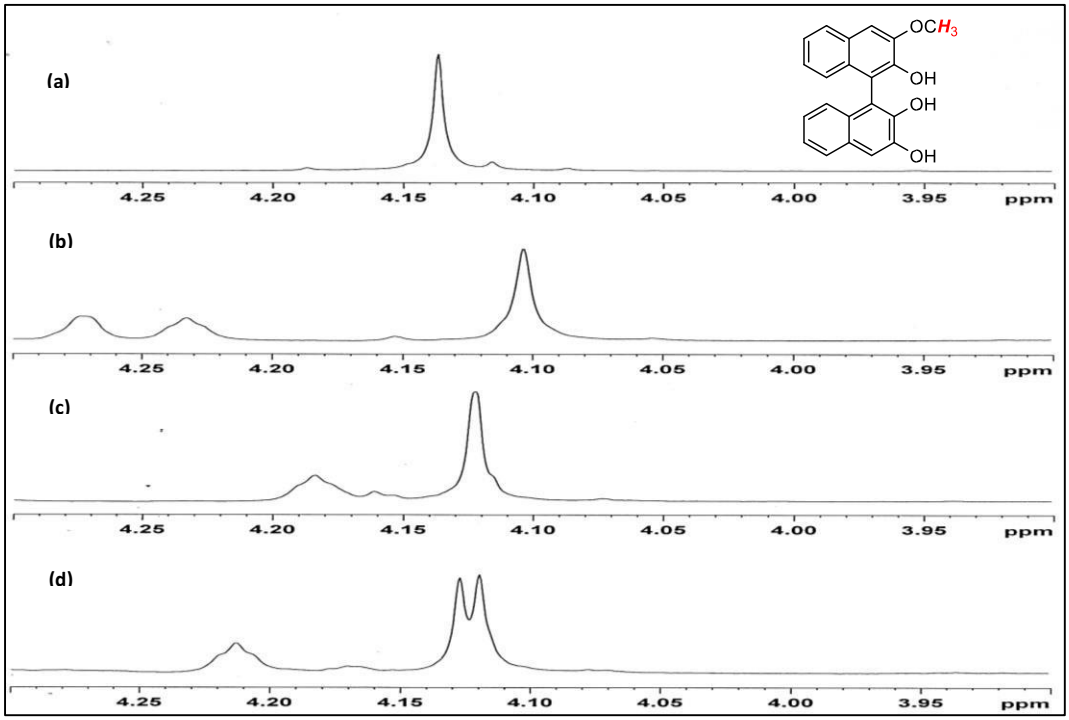

Figure 27: ^{1}H NMR Spectra of: (a) (±) 3-methoxy-2,2,'3'-trihydroxy-1,1'-binaphthyl (b) (±) 3-methoxy-2,2,'3'-trihydroxy-1,1'-binaphthyl & *(R)*-**2** (c) (±) 3-methoxy-2,2,'3'-trihydroxy-1,1'-binaphthyl & *(R,R)*-**3** (d) (±) 3-methoxy-2,2,'3'-trihydroxy-1,1'-binaphthyl & *(R,S)*-**3**

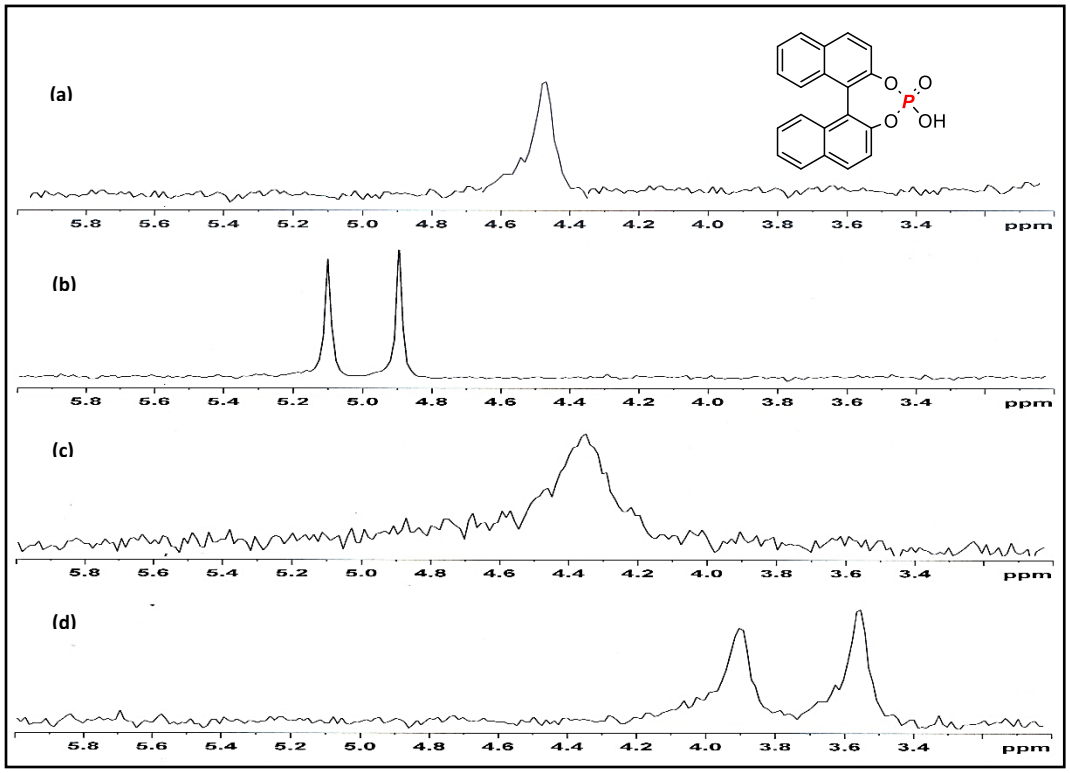

Figure 28: ^{31}P NMR Spectra of: (a) (±) 1,1′-Binaphthyl-2,2′-diyl hydrogenphosphate (b) (±) 1,1′-Binaphthyl-2,2′-diyl hydrogenphosphate & *(R)*-**2** (c) (±) 1,1′-Binaphthyl-2,2′-diyl hydrogenphosphate & *(R,R)*-**3** (d) (±)1,1′-Binaphthyl-2,2′-diyl hydrogenphosphate & *(R,S)*-**3**

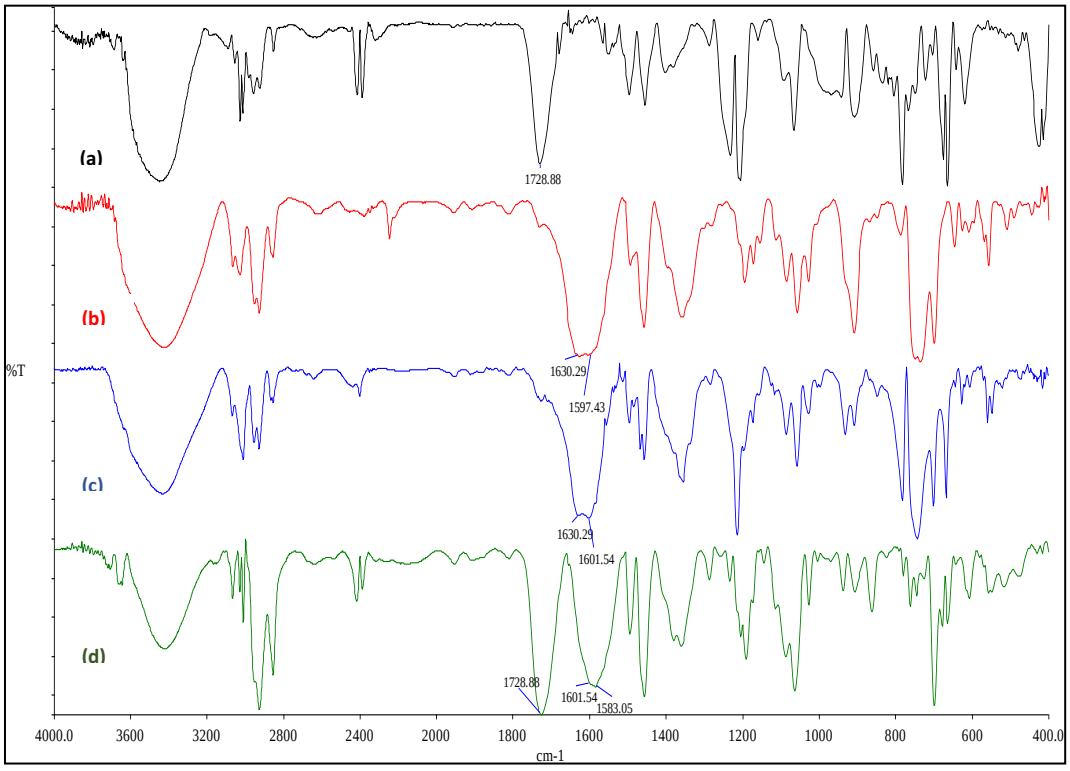

Figure 29: IR Spectra of: (a) (±) Mandelic acid (b) (±) Mandelic acid & *(R)*-**2** (c) (±) Mandelic acid & *(R,R)*-**3** (d) (±) Mandelic acid & *(R,S)*-**3**

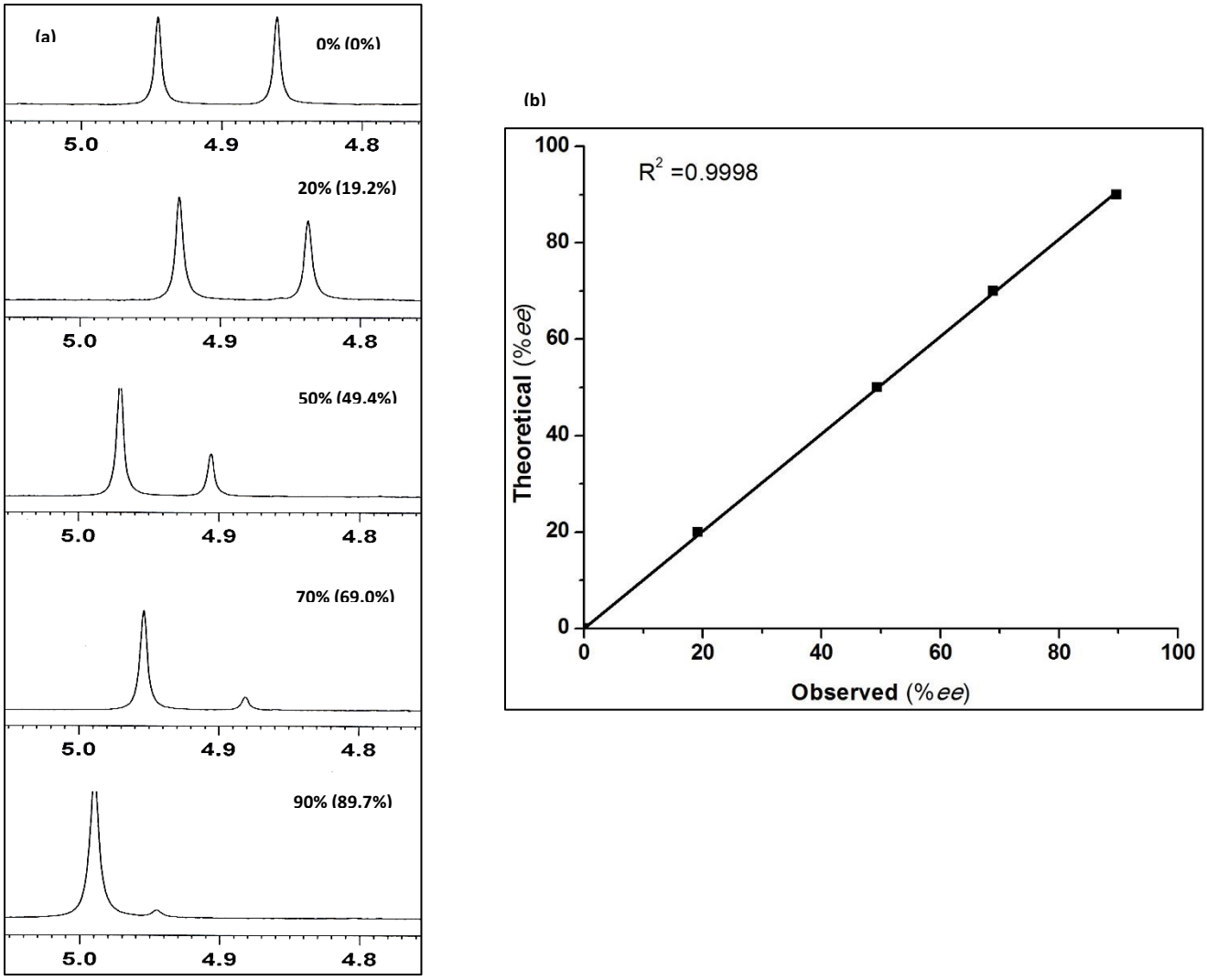

Figure 30: (a) Selected region of ^{1}H NMR spectra of (±) Mandelic acid of various ratios of optical purity in the presence of *(R)*-**2.** Values in parenthesis are observed purity. (b) Correlation between theoretical and observed *ee* values.

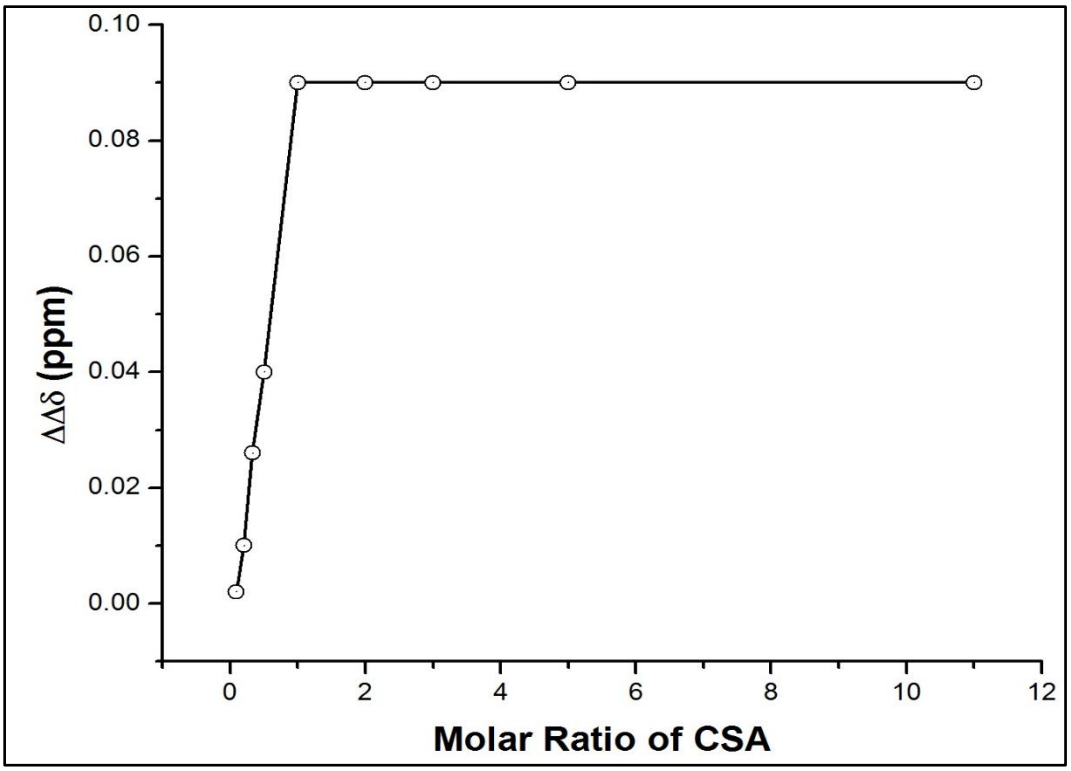

Figure **31**: Graph of ^{1}H NMR titration experiment showing the effect of very low molar ratio of (*R,R*-**3**) to excess of (*R,R*-**3**) on chemical shift nonequivalence for α-*H* proton of Mandelic acid

In this set of experiment, the molar concentration of *rac*-Mandelic acid and (*R,R)*-**3** was varied such that the ratio of their concentration is 0.09, 0.20, 0.33, 0.50, 1.00, 2.00, 3.00, 5.00 and 11.00. The ^{1}H NMR spectrum was recorded and chemical shift nonequivalence (ΔΔδ) in each case was noted. The observed ΔΔδ was plotted against the molar ratio of (*R,R)*-**3**. The graph clearly shows a drastic increase in the value of ΔΔδ on gradual increase in the mole ratio of *R,R*-**3**, till a maximum is reached where the ratio of the concentration of *rac*-Mandelic acid to (*R,R)*-**3** is 1.0 after which there is negligible change in the value of ΔΔδ even on adding large excess of (*R,R)*-**3**. Hence 1.0 equivalent of (*R,R)*-**3** is sufficient to bring maximum separation of the peaks for α-*H* proton of the two enantiomers of Mandelic acid.

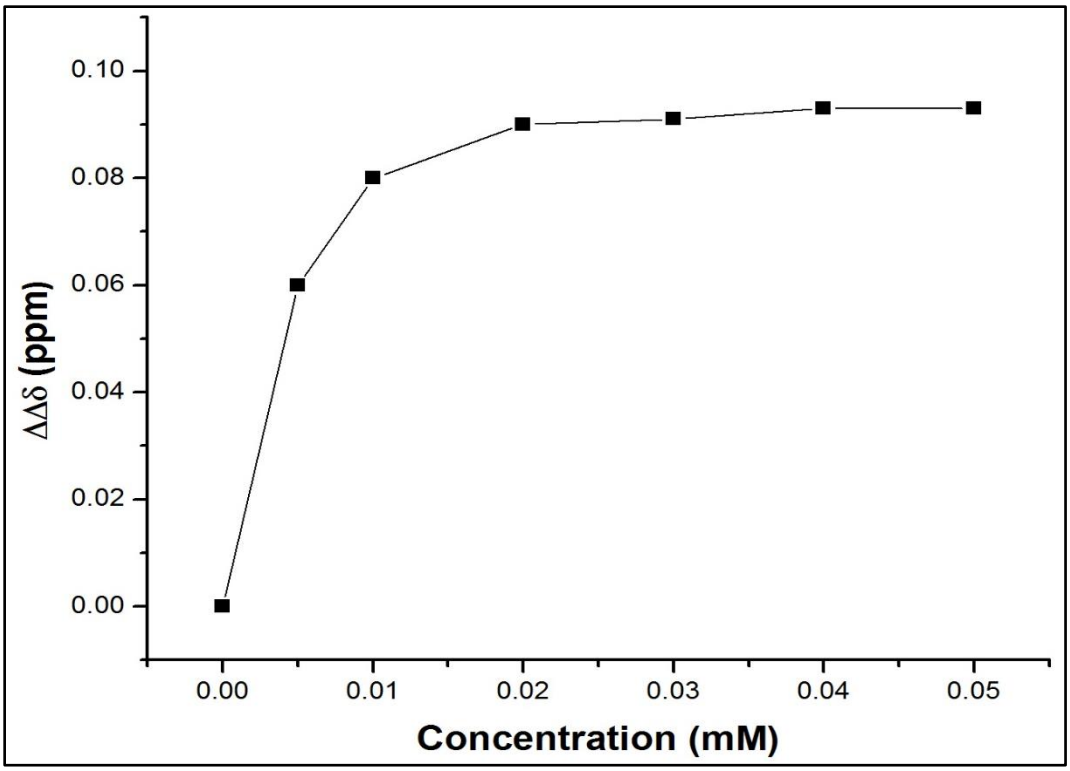

Figure **32**: Graph showing change in chemical shift nonequivalence for α-*H* proton of Racemic Mandelic acid at different concentrations having 1:1 molar ratio with (*R,R*-**3**)

The concentration of *rac*-Mandelic acid and (*R,R)*-**3** is varied keeping their molar ratio constant at 1.0. The ^{1}H NMR was recorded at different concentrations of 5mM, 10mM, 20mM, 30mM, 40mM and 50mM. The observed ΔΔδ was plotted against the increase in concentration. We observed large increase in the value of ΔΔδ as the concentration was increased from 5mM to 20mM. However, there was not much increase in the value of ΔΔδ when the concentration changes from 20mM to 50mM. Hence at a concentration of 20mM for *rac*-Mandelic acid and (*R,R)*-**3**, the value of ΔΔδ is maximum indicating maximum separation of the peaks for α-*H* proton of the two enantiomers of Mandelic acid.

Table 1: A-**1** toA-**7** are some chiral amines known for their CSA activity in the literature. Table shows a comparison of the literature values of induced chemical shift for some of the substrates with our CSAs.

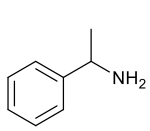

A-1

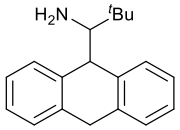

A-2

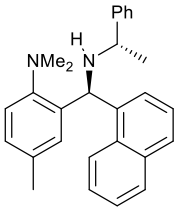

A-3

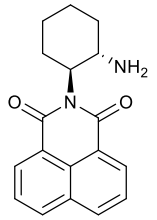

A-4

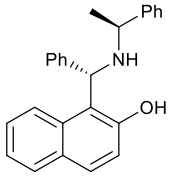

A-5

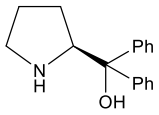

A-6

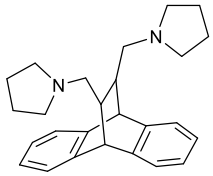

A-7

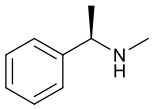

A-8

Sr. No.	Substrate	Our Best CSA	ΔΔδ	Reported CSA	ΔΔδ
1.	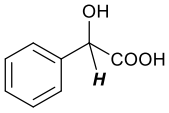	*R*-**2**	0.123	A-**1**[a]	0.035
				A-**3**[a]	0.085
				A-**5**[d]	0.025
				A-**6**[e]	0.062
				A-**7**[f]	0.071
				A-**8**	--
2.	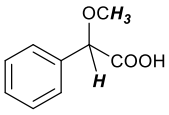	*R,R*-**3**	0.043 (αH) 0.049 (CH_3)	A-**2**[b]	0.014 (αH)
				A-**3**[a]	0.021 (CH_3)
				A-**4**[c]	0.051 (αH)
				A-**6**[e]	0.023 (αH)
					0.003 (CH_3)
3.	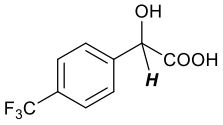	*R*-**2**	0.077	A-**5**[d]	0.056
4.	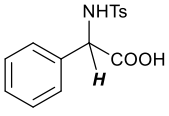	*R,R*-**3**	0.070	A-**1**[a]	0.031
5.	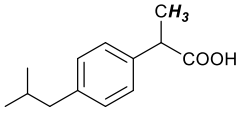	*R,R*-**3**	0.019	A-**2**[b]	0.005

References:

(a) Wang, W.; Ma, F.; Shen, X.; Zhang, C. *Tetrahedron: Asymmetry* **2007**, *18*, 832.

(b) Port, A.; Virgili, A.; Jaime, C. *Tetrahedron: Asymmetry* **1996**, *7*, 1295.

(c) Yang, X.; Wang, G.; Zhong, C.; Wua, X.; Fua, E. *Tetrahedron: Asymmetry* **2006**, *17*, 916

(d) Chaudhary, a.; Yadav, P.; Bedekar, A. *Tetrahedron: Asymmetry* **2014**, *25*, 767

(e) Li, G.; Cao, J.; Zong, W.; Lei, X.; Tan, R.; *Org. Chem. Front*. **2016**, *3*, 96

(f) Jain, N.; Mandal, M.; Bedekar, A. *Tetrahedron* **2014**, *70*, 4343

X-ray Crystal Structure for RR-R-MA: (CCDC No. 1468129)

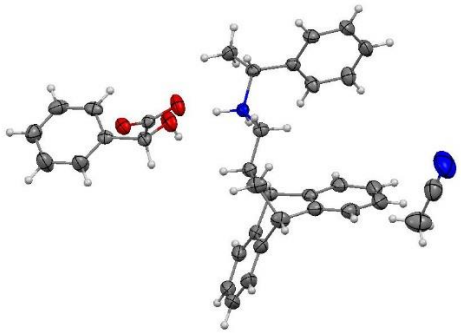

(50% probability factor for thermal ellipsoids)

Table 2: Crystal data and structure refinement for R_R_R_MA_0m (1)

Empirical formula	$C_{17.5}H_{18}NO_{1.5}$
Formula weight	266.33
Formula weight	266.33
Temperature/K	296(2)
Crystal system	Monoclinic
Space group	P21
a/Å	10.8811(8)
b/Å	9.6564(7)
c/Å	14.0641(11)
α/°	90
β/°	97.8640(10)
γ/°	90
Volume/Å3	1463.85(19)
Z	4
ρ_{calc}g/cm3	1.208
μ/mm-1	0.077

F(000)	568.0
Radiation	MoKα (λ = 0.71073)
2Θ range for data collection/°	3.778 to 49.992
Index ranges	-12 ≤ h ≤ 12, -11 ≤ k ≤ 11, -16 ≤ l ≤ 16
Reflections collected	15313
Independent reflections	5161 [Rint = 0.0283, Rsigma = 0.0288]
Data/restraints/parameters	5161/1/364
Goodness-of-fit on F2	1.071
Final R indexes [I>=2σ (I)]	R1 = 0.0368, wR2 = 0.0873
Final R indexes [all data]	R1 = 0.0399, wR2 = 0.0887
Largest diff. peak/hole / e Å-3	0.12/-0.17

Table 3: Fractional Atomic Coordinates (×10^4) and Equivalent Isotropic Displacement Parameters (Å^2×10^3) for R_R_R_MA_0m (1). U_{eq} is defined as 1/3 of of the trace of the orthogonalised U_{IJ} tensor.

Atom	*x*	*y*	*z*	U(eq)
O2	8251.0(15)	-1403.0(17)	554.1(13)	34.7(4)
C1	6077(2)	1293(3)	8380.8(19)	42.3(7)
C2	5155(2)	2259(3)	8426.7(19)	41.3(6)
C3	4120(2)	1934(3)	8852.6(18)	35.0(6)
C4	3978(2)	618(3)	9218.1(16)	28.3(5)
C5	2912(2)	246(3)	9754.0(17)	30.5(5)
N1	1680.0(16)	765(2)	9271.2(13)	25.6(4)
C7	1298(2)	171(3)	8296.8(17)	30.1(5)
C8	44(2)	728(3)	7834.9(17)	31.5(5)
C9	129(2)	2201(3)	7391.1(16)	30.1(5)
C10	847(2)	2072(3)	6549.3(17)	31.2(5)
C11	1925(2)	2779(3)	6428(2)	39.4(6)
C12	2453(3)	2583(4)	5596(2)	52.0(8)
C13	1938(3)	1650(4)	4908(2)	57.5(9)
C14	313(2)	1151(3)	5844.9(18)	37.0(6)
C15	-875(2)	513(3)	6079.3(19)	40.6(6)
C16	-537(3)	-281(3)	7030.5(19)	42.7(7)
C17	-1725(2)	1692(3)	6276.6(17)	37.5(6)
C18	-2930(2)	1928(4)	5837.9(19)	47.4(8)
C19	-3557(3)	3089(4)	6092(2)	52.8(9)
C20	-3013(3)	4007(4)	6773(2)	49.1(8)
C21	-1821(2)	3762(3)	7232.3(18)	39.4(6)
C22	-1182(2)	2607(3)	6978.1(17)	32.6(6)
C23	879(3)	918(3)	5035(2)	50.1(8)
C24	3104(2)	816(3)	10772.5(17)	40.9(6)
C25	4908(2)	-355(3)	9155.2(18)	36.9(6)

C26	5953(2)	-24(3)	8747.6(19)	43.4(7)
C27	4256(4)	9760(4)	6374(3)	74.5(11)
C28	5222(4)	8741(4)	6435(3)	63.4(9)
N2	5976(4)	7919(5)	6491(3)	102.7(13)
C30	9103(2)	-603(2)	416.7(16)	27.3(5)
C31	8925(2)	945(2)	631.1(18)	30.4(5)
C32	8257(2)	1155(2)	1500.9(17)	28.8(5)
C33	6982(2)	1137(3)	1412(2)	44.4(7)
C34	6373(3)	1321(4)	2201(2)	54.9(8)
C35	7039(3)	1520(3)	3098.6(19)	48.8(7)
O3	10079.7(19)	-932.0(19)	93.9(16)	45.7(5)
O1	10097.6(16)	1591(2)	736.0(16)	45.2(5)
C38	8303(3)	1544(3)	3194(2)	45.3(7)
C39	8916(2)	1358(3)	2407.8(19)	37.0(6)

Table 4: Anisotropic Displacement Parameters ($Å^2×10^3$) for R_R_R_MA_0m (1). The Anisotropic displacement factor exponent takes the form: $-2\pi^2[h^2a^{*2}U_{11}+2hka^*b^*U_{12}+\ldots]$.

Atom	U_{11}	U_{22}	U_{33}	U_{23}	U_{13}	U_{12}
O2	32.2(9)	24.2(9)	49.1(10)	-0.2(8)	10.1(8)	-2.6(8)
C1	27.3(12)	61.1(19)	39.7(14)	-1.7(14)	8.1(10)	-2.2(13)
C2	39.9(14)	38.2(16)	48.2(15)	-1.2(13)	14.5(12)	-6.5(13)
C3	32.7(13)	28.5(14)	45.7(15)	-2.8(11)	11.8(11)	1.0(11)
C4	26.1(11)	30.3(13)	27.6(12)	-1.3(10)	0.3(9)	0.1(10)
C5	27.5(12)	26.5(12)	36.8(12)	8.9(10)	1.5(10)	2.2(10)
N1	25.0(9)	22.7(10)	29.7(10)	2.3(8)	6.2(8)	-1.0(8)
C7	33.5(13)	24.4(12)	31.9(12)	-0.9(10)	2.1(10)	0.0(11)
C8	30.1(12)	31.3(13)	32.6(12)	1.7(11)	2.4(10)	-2.4(11)
C9	30.5(12)	29.7(13)	29.3(12)	-0.6(10)	1.5(9)	-0.1(11)
C10	30.0(12)	27.0(13)	35.6(13)	4.3(10)	1.6(10)	5.8(10)
C11	33.2(13)	36.2(15)	48.2(15)	9.6(12)	3.7(11)	5.0(12)
C12	39.6(15)	58(2)	62.0(19)	20.5(16)	18.7(14)	10.7(15)
C13	50.4(18)	79(2)	45.7(17)	13.3(17)	17.5(14)	27.6(18)
C14	37.6(13)	40.1(16)	32.2(13)	-0.7(11)	0.4(10)	9.0(11)
C15	41.1(14)	39.0(16)	39.0(14)	-8.8(12)	-4.1(11)	-3.0(12)
C16	44.0(16)	33.2(15)	47.1(15)	-0.9(13)	-7.3(12)	-8.5(12)
C17	33.1(13)	48.3(16)	30.6(13)	6.7(12)	2.8(10)	-2.9(12)
C18	35.9(14)	70(2)	35.0(14)	9.4(14)	0.1(11)	-4.7(14)
C19	31.1(14)	85(3)	43.5(16)	21.9(17)	7.7(12)	12.3(15)
C20	41.9(15)	63(2)	44.7(16)	18.2(15)	15.3(13)	17.8(15)
C21	40.3(14)	43.0(16)	37.1(14)	6.7(12)	12.9(11)	5.3(13)
C22	32.9(12)	37.6(15)	28.3(12)	6.8(11)	7.7(10)	0.7(11)
C23	49.9(17)	62(2)	37.3(14)	-4.8(14)	1.3(12)	19.7(15)

C24	36.1(13)	55.2(17)	30.7(13)	7.8(12)	1.2(10)	-1.6(13)
C25	35.8(14)	35.8(14)	38.3(14)	4.5(11)	2.8(11)	8.2(12)
C26	32.5(14)	56(2)	43.1(14)	3.4(14)	8.6(12)	14.1(13)
C27	76(2)	61(2)	82(3)	-8(2)	-5(2)	14(2)
C28	66(2)	66(2)	61(2)	-1.9(18)	23.2(17)	3(2)
N2	92(3)	101(3)	125(3)	2(2)	52(2)	32(3)
C30	30.3(13)	23.7(13)	28.0(12)	4.4(10)	3.9(10)	-0.4(10)
C31	31.0(12)	23.0(13)	38.3(13)	5.3(10)	8.9(10)	0.8(10)
C32	33.2(12)	18.8(12)	34.0(12)	0.5(10)	3.1(10)	1.3(10)
C33	34.1(13)	61(2)	37.2(14)	-12.5(13)	2.1(11)	0.5(13)
C34	36.1(14)	78(2)	51.5(17)	-14.1(16)	10.9(13)	0.0(16)
C35	58.0(18)	54.6(19)	35.8(15)	-1.8(14)	13.7(13)	9.3(16)
O3	42.5(10)	28.4(10)	72.6(13)	-3.3(9)	31.3(9)	-1.2(8)
O1	39.7(10)	25.7(9)	73.7(14)	2.1(9)	20.7(9)	-8.3(8)
C38	57.9(17)	42.4(16)	32.7(14)	-1.2(12)	-4.7(12)	12.8(14)
C39	35.0(13)	27.3(14)	46.5(15)	-1.1(12)	-2.0(11)	4.1(11)

Table 5: Bond Lengths for R_R_R_MA_0m (1).

Atom	Atom	Length/Å	Atom	Atom	Length/Å
O2	C30	1.242(3)	C15	C17	1.516(4)
C1	C2	1.378(4)	C15	C16	1.542(4)
C1	C26	1.385(4)	C17	C18	1.390(4)
C2	C3	1.382(3)	C17	C22	1.394(4)
C3	C4	1.386(4)	C18	C19	1.384(5)
C4	C25	1.393(3)	C19	C20	1.378(5)
C4	C5	1.511(3)	C20	C21	1.388(4)
C5	N1	1.503(3)	C21	C22	1.387(4)
C5	C24	1.522(4)	C25	C26	1.380(4)
N1	C7	1.491(3)	C27	C28	1.434(5)
C7	C8	1.526(3)	C28	N2	1.137(5)
C8	C16	1.560(4)	C30	O3	1.252(3)
C8	C9	1.562(4)	C30	C31	1.543(3)
C9	C10	1.511(3)	C31	O1	1.410(3)
C9	C22	1.515(3)	C31	C32	1.519(3)
C10	C11	1.387(4)	C32	C33	1.376(4)
C10	C14	1.397(4)	C32	C39	1.389(3)
C11	C12	1.385(4)	C33	C34	1.379(4)
C12	C13	1.383(5)	C34	C35	1.380(4)
C13	C23	1.384(5)	C35	C38	1.364(4)
C14	C23	1.386(4)	C38	C39	1.379(4)
C14	C15	1.509(4)			

Table 6: Bond Angles for R_R_R_MA_0m (1).

Atom	Atom	Atom	Angle/°	Atom	Atom	Atom	Angle/°
C2	C1	C26	119.7(2)	C15	C16	C8	110.1(2)
C1	C2	C3	120.6(3)	C18	C17	C22	119.5(3)
C2	C3	C4	120.5(2)	C18	C17	C15	127.2(3)
C3	C4	C25	118.5(2)	C22	C17	C15	113.3(2)
C3	C4	C5	122.3(2)	C19	C18	C17	119.1(3)
C25	C4	C5	119.0(2)	C20	C19	C18	121.3(3)
N1	C5	C4	113.16(18)	C19	C20	C21	119.9(3)
N1	C5	C24	107.69(19)	C22	C21	C20	119.2(3)
C4	C5	C24	111.6(2)	C21	C22	C17	120.9(2)
C7	N1	C5	113.96(18)	C21	C22	C9	126.0(2)
N1	C7	C8	112.10(19)	C17	C22	C9	113.1(2)
C7	C8	C16	109.8(2)	C13	C23	C14	119.6(3)
C7	C8	C9	113.14(19)	C26	C25	C4	121.1(3)
C16	C8	C9	108.63(19)	C25	C26	C1	119.7(3)
C10	C9	C22	106.36(18)	N2	C28	C27	178.9(4)
C10	C9	C8	107.65(19)	O2	C30	O3	126.0(2)
C22	C9	C8	106.56(19)	O2	C30	C31	117.1(2)
C11	C10	C14	120.1(2)	O3	C30	C31	116.9(2)
C11	C10	C9	126.4(2)	O1	C31	C32	112.5(2)
C14	C10	C9	113.5(2)	O1	C31	C30	108.23(19)
C12	C11	C10	119.5(3)	C32	C31	C30	111.93(19)
C13	C12	C11	120.2(3)	C33	C32	C39	118.2(2)
C12	C13	C23	120.5(3)	C33	C32	C31	120.8(2)
C23	C14	C10	119.8(3)	C39	C32	C31	121.0(2)
C23	C14	C15	127.1(3)	C32	C33	C34	121.0(3)
C10	C14	C15	113.0(2)	C33	C34	C35	120.2(3)
C14	C15	C17	107.2(2)	C38	C35	C34	119.3(3)
C14	C15	C16	106.4(2)	C35	C38	C39	120.7(3)
C17	C15	C16	107.1(2)	C38	C39	C32	120.6(2)

Table 7: Hydrogen Atom Coordinates (Å×10^4) and Isotropic Displacement Parameters (Å^2×10^3) for R_R_R_MA_0m (1).

Atom	*x*	*y*	*z*	U(eq)
H1	6779	1524	8105	51
H2	5229	3137	8169	50
H3	3514	2602	8894	42
H5	2869	-766	9792	37
H1A	1050	546	9674	31

H1B	1718	1765	9218	31
H7A	1251	-829	8346	36
H7B	1922	391	7889	36
H8	-510	776	8328	38
H9	506	2874	7865	36
H11	2290	3379	6901	47
H12	3157	3082	5499	62
H13	2306	1514	4357	69
H15	-1260	-92	5563	49
H16A	51	-1011	6944	51
H16B	-1276	-705	7217	51
H18	-3311	1315	5380	57
H19	-4362	3253	5797	63
H20	-3444	4791	6924	59
H21	-1456	4364	7705	47
H23	549	274	4579	60
H24A	2403	581	11087	61
H24B	3189	1805	10752	61
H24C	3842	421	11120	61
H25	4822	-1244	9392	44
H26	6572	-681	8719	52
H27A	3816	9674	6919	112
H27B	3691	9621	5795	112
H27C	4613	10669	6367	112
H31	8415	1357	74	36
H33	6524	998	812	53
H34	5510	1310	2128	66
H35	6630	1638	3632	59
H1C	10038	2350	472	68
H38	8757	1687	3796	54
H39	9779	1369	2485	44

Discussion of the X-Ray Crystal Structure of RR-R-MA:

The complex [(*R*,*R*)-**3**•*S*-MA] also crystallized in monoclinic chiral $P2_1$ space group containing two molecules of each components in the asymmetric unit. The crystal structure of [(*R*,*R*)-**3**•*S*-MA] (Figure 5) is isostructural to the [(*R*,*R*)-**3**•*R*-MA] structure. The C–O bond lengths (~1.24-1.26 Å) in the COOH group show that proton transfer has occurred from *S*-MA to amine moiety of the (*R*,*R*)-**3** revealing that the complex is salt. The neighboring symmetry independent *S*-MA molecules generate the helical chain similar to [(*R*,*R*)-**3**•*R*-MA] through O-H···O

hydrogen bond (H···O = 1.907 Å, O…O = 2.720 Å /O-H···O = 163° and H···O = 1.598 Å, O···O = 2.827 Å /O-H···O = 155°) involving hydroxyl H-atom and carbonyl oxygen of the carboxylic group having graph set notation $C_2^2(10)$, wherein C(10) denotes a chain motif with ten atoms in the repeat unit. Both symmetry independent (*R*,*R*)-**3** molecules are associated with this extended chain on either side through N-H···O hydrogen bonding interactions to generate the layered structure. One of the N-H proton of (*R*,*R*)-**3** is involved in the bifurcated N-H···O hydrogen bonding interactions with the carbonyl (H···O = 1.925 Å, N···O = 2.739 Å /O-H···O = 138°; H…O = 1.901 Å, N···O = 2.729 Å /O-H···O = 137°) and hydroxyl (H···O = 2.013 Å, N···O = 2.818 Å /O-H···O = 138°; H···O = 2.059 Å, N···O = 2.878 Å /O-H···O = 139°) oxygens of *S*-MA molecules with graph set notation $[R_1^2(5)]$ representing hydrogen bonding ring motif consisting of five atoms, with one donor group and two acceptor groups. The other N-H proton forms a N-H···O hydrogen bonding interactions with the carboxyl oxygen of *S*-MA (H···O = 1.821 Å, N···O = 2.788 Å /O-H···O = 165°; H···O = 1.959 Å, N···O = 2.916 Å /O-H···O = 162°) with graph set notation [D(2)] representing hydrogen bonding finite motif consisting of two atoms. Similar to the crystal structure of [(*R*,*R*)-**3**•*R*-MA], two molecules of each *S*-MA and (*R*,*R*)-**3** constitute a tetrameric structure through hydrogen bonding interactions which is extended along the *a*-axis to generate the chain structure. The neighboring chains are loosely connected to each other roughly along the *b*-axis *via* hydrophobic interactions. To the best of our knowledge there are very few reports on the crystal study of the structure of the salt of test substrate and the CSA to understand the supramolecular interactions. The experimental observations of shielding and deshielding effects in the two pairs in ^{1}H NMR analysis corroborated well with the information obtained from these crystal structures, even though one needs to be cautious to compare the two.

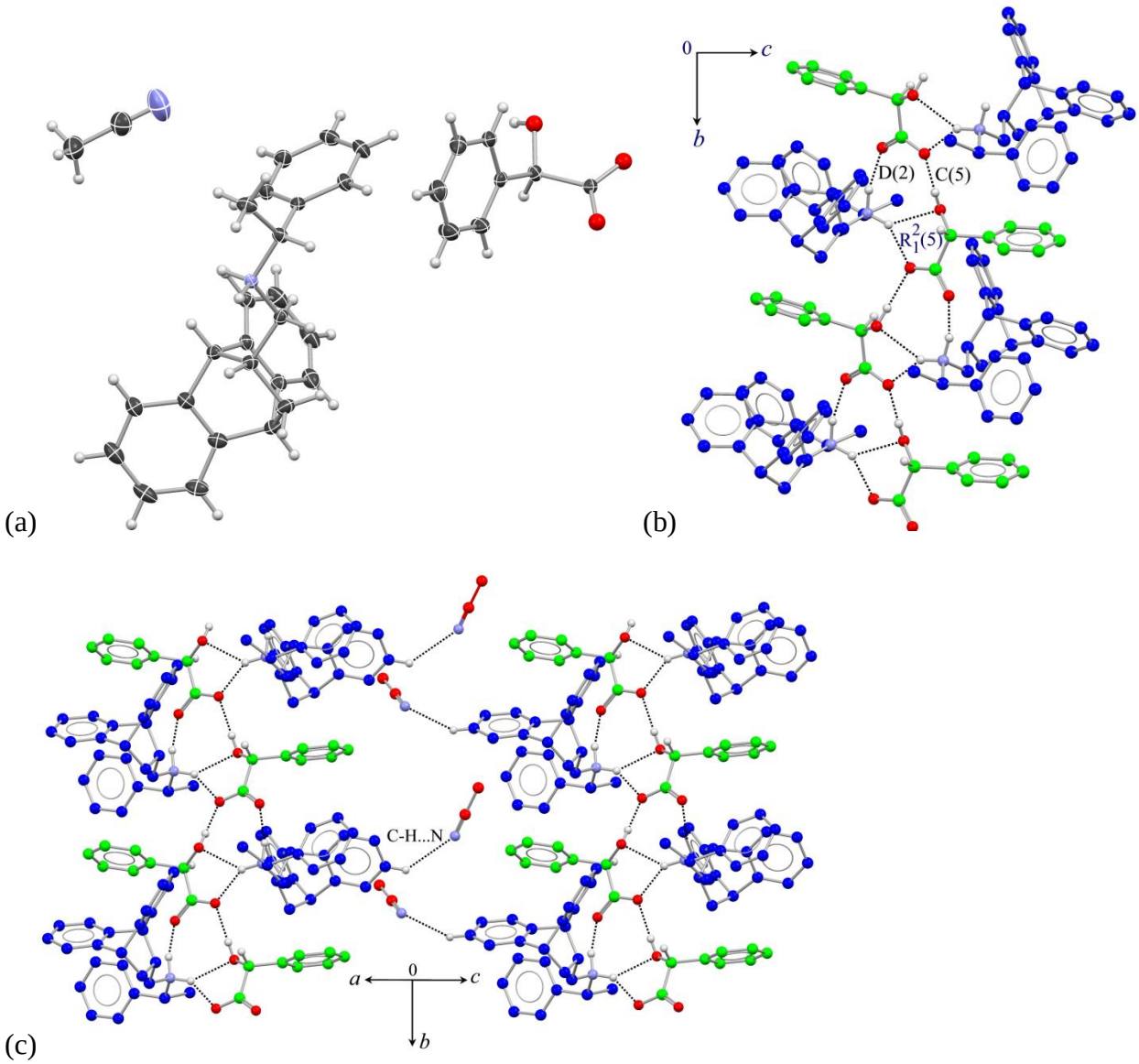

Figure 33 (a) ORTEP view of (*R*,*R*)-**3**•*R*-MA salt. The displacement ellipsoids are drawn at 30% probability level and H atoms are shown as small spheres of arbitrary radii. (b) Association of the (*R*,*R*)-**3** (blue) molecules to the O-H···O hydrogen bonded helical chain of *R*-MA (green) through N-H···O hydrogen bonding interactions generating an extended chain assembly. (c) linking of the neighboring helical chains through acetonitrile molecules via C-H···N interactions.

X-ray Crystal Structure for RR-S-MA: (CCDC 1468131)

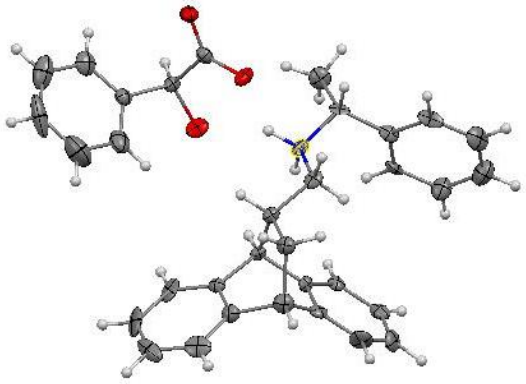

(50% probability factor for thermal ellipsoids)

Table 8: Crystal data and structure refinement for RR_S_MA_0m (1).

Identification code	RR_S_MA_0m (1)
Empirical formula	$C_{33}H_{33}NO_3$
Formula weight	491.60
Temperature/K	150(2)
Crystal system	Monoclinic
Space group	$P2_1$
a/Å	9.7297(14)
b/Å	24.373(4)
c/Å	12.012(2)
α/°	90
β/°	92.421(7)
γ/°	90
Volume/Å^3	2846.1(8)
Z	4
ρ_{calc}g/cm^3	1.147
μ/mm^{-1}	0.073
F(000)	1048.0
Crystal size/mm^3	0.360 × 0.310 × 0.210
Radiation	MoKα (λ = 0.71073)
2Θ range for data collection/°	3.342 to 49.998
Index ranges	$-11 \leq h \leq 11$, $-27 \leq k \leq 28$, $-12 \leq l \leq 12$
Reflections collected	13867
Independent reflections	7860 [R_{int} = 0.0689, R_{sigma} = 0.1541]
Data/restraints/parameters	7860/181/671
Goodness-of-fit on F^2	1.075

Final R indexes [I>=2σ (I)]	R_1 = 0.0991, wR_2 = 0.1307
Final R indexes [all data]	R_1 = 0.1501, wR_2 = 0.1486
Largest diff. peak/hole / e Å^{-3}	0.28/-0.30

Table 9: Fractional Atomic Coordinates (×10^4) and Equivalent Isotropic Displacement Parameters (Å^2×10^3) for RR_S_MA_0m (1). U_{eq} is defined as 1/3 of of the trace of the orthogonalised U_{IJ} tensor.

Atom	*x*	*y*	*z*	U(eq)
O1	4927(6)	4882(3)	2824(6)	25.4(18)
O2	4491(6)	5557(2)	4001(5)	18.8(16)
O3	7393(6)	5266(2)	2454(6)	24.5(18)
N1	6440(8)	4295(3)	11365(7)	14.9(19)
C1	7550(10)	5092(4)	9582(8)	18(2)
C2	6082(9)	5072(4)	10037(8)	16(2)
C3	5037(10)	5341(4)	9173(9)	28(3)
C4	5866(10)	5619(4)	8244(9)	26(3)
C5	6946(10)	5993(4)	8784(9)	22(3)
C6	7858(9)	5708(4)	9489(8)	16(2)
C7	8891(10)	5977(4)	10097(9)	28(3)
C8	9049(12)	6545(4)	9983(10)	37(3)
C9	8115(13)	6824(4)	9266(11)	42(4)
C10	7060(13)	6551(5)	8665(11)	42(3)
C11	7486(10)	4865(4)	8394(9)	21(3)
C12	6570(10)	5155(4)	7691(9)	24(3)
C13	6393(11)	4995(4)	6575(10)	35(3)
C14	7119(12)	4541(4)	6207(11)	39(3)
C15	7999(11)	4258(4)	6907(10)	30(3)
C16	8180(10)	4408(4)	8043(9)	26(3)
C17	5655(10)	4487(4)	10333(8)	19(2)
C18	6006(10)	3758(4)	11825(8)	19(2)
C19	6820(11)	3661(4)	12908(9)	30(3)
C20	6187(10)	3302(4)	10972(9)	21(3)
C21	7438(11)	3191(4)	10558(9)	28(3)
C22	7599(14)	2764(5)	9800(11)	52(4)
C23	6482(16)	2455(5)	9480(11)	56(4)
C24	5218(16)	2560(5)	9866(11)	55(4)
C25	5009(12)	2998(4)	10633(10)	39(3)
C26	5289(10)	5291(4)	3424(8)	17(2)
C27	6801(9)	5461(3)	3437(9)	18(3)
C28	6991(9)	6080(4)	3549(9)	18(2)
C29	7102(10)	6315(4)	4603(10)	28(3)
C30	7265(11)	6878(5)	4730(12)	44(4)
C31	7284(11)	7212(5)	3797(14)	54(4)

C32	7161(10)	6979(5)	2745(12)	43(4)
C33	7000(10)	6413(4)	2626(10)	34(3)
O1'	-59(6)	4961(3)	2568(6)	26.5(18)
O2'	-559(7)	4285(3)	1365(6)	24.4(18)
O3'	2313(6)	4565(3)	3225(6)	25.4(19)
N1'	1668(7)	5699(3)	3608(6)	17(2)
C1'	2439(9)	5364(3)	6010(8)	15(2)
C2'	921(9)	5423(4)	5507(8)	17(2)
C3'	-20(9)	5592(4)	6468(8)	23(3)
C4'	881(10)	5647(4)	7593(9)	27(3)
C5'	1577(10)	5093(4)	7782(9)	22(3)
C6'	2385(9)	4939(4)	6911(8)	18(2)
C7'	3060(10)	4446(4)	6958(10)	28(3)
C8'	2896(12)	4093(4)	7868(11)	40(4)
C9'	2096(12)	4257(5)	8732(11)	42(4)
C10'	1423(10)	4761(4)	8706(10)	34(3)
C11'	2798(9)	5924(3)	6512(8)	16(2)
C12'	1966(10)	6069(4)	7383(9)	20(3)
C13'	2126(12)	6567(4)	7891(9)	32(3)
C14'	3116(11)	6937(4)	7538(10)	31(3)
C15'	3922(10)	6798(4)	6646(9)	27(3)
C16'	3772(9)	6288(4)	6137(9)	18(3)
C17'	822(10)	5852(4)	4571(9)	22(3)
C18'	1494(9)	6088(4)	2630(8)	17(2)
C19'	2365(10)	5866(4)	1680(9)	30(3)
C20'	1909(9)	6666(4)	2948(9)	20(3)
C21'	927(10)	7083(4)	2772(9)	26(3)
C22'	1303(12)	7626(5)	3009(10)	38(3)
C23'	2586(13)	7759(5)	3435(11)	42(4)
C24'	3533(11)	7345(4)	3654(10)	33(3)
C25'	3203(10)	6797(4)	3382(8)	22(3)
C26'	191(10)	4517(4)	2085(9)	21(3)
C27'	1553(9)	4224(4)	2474(9)	17(2)
C28'	1142(11)	3690(4)	3028(10)	23(3)
C29'	859(10)	3235(4)	2413(10)	34(3)
C30'	369(12)	2763(5)	2892(14)	52(4)
C31'	116(13)	2761(5)	4019(15)	66(5)
C32'	425(14)	3224(6)	4655(13)	68(5)
C33'	972(11)	3690(5)	4155(11)	40(3)

Table 10: Anisotropic Displacement Parameters ($Å^2 \times 10^3$) for RR_S_MA_0m (1). The Anisotropic displacement factor exponent takes the form: $-2\pi^2[h^2a^{*2}U_{11}+2hka^*b^*U_{12}+\ldots]$.

Atom	U_{11}	U_{22}	U_{33}	U_{23}	U_{13}	U_{12}
O1	21(3)	28(3)	27(3)	-5(2)	6(2)	-2(2)
O2	14(2)	20(2)	22(3)	-5(2)	6(2)	2(2)
O3	24(4)	21(4)	29(5)	-7(3)	6(4)	-4(3)
N1	12(3)	16(3)	16(4)	-1(3)	-1(3)	-2(3)
C1	14(4)	20(4)	18(4)	5(3)	3(3)	0(3)
C2	13(4)	18(4)	16(4)	0(3)	5(3)	1(3)
C3	23(6)	31(6)	31(8)	-5(5)	7(6)	4(5)
C4	20(6)	27(6)	29(8)	11(5)	-13(5)	-4(5)
C5	11(6)	29(6)	25(8)	6(5)	7(5)	5(5)
C6	6(5)	25(6)	19(7)	-3(5)	7(5)	-3(4)
C7	23(7)	43(7)	19(8)	-1(6)	10(6)	-11(5)
C8	27(7)	44(8)	39(9)	-8(6)	10(7)	-20(6)
C9	44(8)	22(7)	61(11)	-6(7)	16(8)	-5(6)
C10	43(8)	40(8)	42(10)	8(7)	4(7)	-2(6)
C11	18(4)	22(4)	22(4)	1(3)	2(3)	1(3)
C12	22(4)	27(4)	23(4)	0(3)	1(3)	-7(3)
C13	34(4)	35(4)	36(5)	4(4)	3(4)	-9(3)
C14	39(4)	40(4)	39(5)	-2(4)	3(4)	-13(4)
C15	33(4)	25(4)	34(5)	-5(3)	8(4)	-8(3)
C16	23(4)	27(4)	28(4)	1(3)	3(3)	-4(3)
C17	18(4)	19(4)	20(4)	0(3)	1(3)	0(3)
C18	14(4)	20(4)	22(4)	-2(3)	4(3)	1(3)
C19	36(6)	29(5)	25(6)	1(5)	5(5)	4(5)
C20	12(6)	29(6)	22(8)	-5(5)	8(5)	0(5)
C21	24(7)	25(6)	35(9)	-3(6)	9(6)	-3(5)
C22	71(11)	30(7)	57(11)	-1(7)	26(9)	2(7)
C23	92(12)	39(8)	39(10)	-15(7)	27(9)	-22(8)
C24	78(11)	43(8)	42(11)	2(7)	-15(9)	-26(8)
C25	44(8)	30(7)	43(10)	10(6)	5(7)	-8(6)
C26	16(4)	15(4)	18(4)	2(3)	4(3)	1(3)
C27	13(4)	22(4)	20(4)	-4(3)	3(3)	2(3)
C28	9(4)	23(4)	21(4)	0(3)	1(3)	-1(3)
C29	25(4)	30(4)	30(4)	-4(3)	4(3)	-1(3)
C30	24(7)	54(9)	54(11)	-27(8)	16(7)	-8(6)
C31	14(7)	39(8)	108(15)	-13(9)	-1(8)	0(6)
C32	12(7)	43(8)	76(12)	13(8)	10(7)	-10(6)
C33	17(6)	36(7)	48(10)	-14(6)	-1(6)	-7(5)
O1'	15(4)	26(4)	37(5)	-13(3)	-8(3)	5(3)
O2'	22(4)	25(4)	26(5)	1(4)	-5(4)	-1(3)
O3'	6(4)	37(4)	33(5)	-7(3)	2(3)	-5(3)
N1'	10(5)	20(4)	22(6)	-4(4)	2(4)	-4(3)
C1'	12(4)	19(4)	15(4)	-3(3)	3(3)	0(3)
C2'	13(4)	21(4)	19(4)	-4(3)	2(3)	0(3)

C3'	18(4)	26(4)	24(4)	1(3)	3(3)	-3(3)
C4'	22(4)	33(4)	28(4)	0(3)	6(3)	0(3)
C5'	18(4)	25(4)	24(4)	1(3)	3(3)	-4(3)
C6'	14(4)	22(4)	19(4)	0(3)	-1(3)	-4(3)
C7'	21(6)	19(6)	44(9)	-8(6)	9(6)	-18(5)
C8'	33(8)	12(6)	75(11)	0(6)	3(8)	-12(5)
C9'	26(7)	49(8)	49(10)	30(7)	-15(7)	-23(6)
C10'	8(6)	54(8)	40(9)	0(7)	1(6)	-10(6)
C11'	12(4)	16(4)	18(4)	-2(3)	2(3)	3(3)
C12'	13(6)	28(6)	19(8)	-1(5)	-7(5)	8(5)
C13'	40(8)	43(7)	14(8)	0(6)	15(6)	4(6)
C14'	30(7)	21(6)	43(9)	-1(6)	-4(7)	16(5)
C15'	19(6)	33(7)	27(8)	8(6)	-9(6)	-9(5)
C16'	10(5)	22(6)	22(8)	1(5)	-5(5)	3(5)
C17'	10(6)	25(6)	31(8)	-5(5)	0(5)	-4(4)
C18'	2(5)	34(6)	13(7)	0(5)	-4(5)	3(4)
C19'	22(6)	37(7)	31(8)	1(6)	12(6)	3(5)
C20'	7(6)	30(6)	23(8)	4(5)	2(5)	4(5)
C21'	4(6)	52(8)	23(8)	10(6)	2(5)	-4(5)
C22'	29(8)	43(8)	42(10)	-1(6)	6(7)	22(6)
C23'	42(9)	34(7)	50(10)	-8(6)	8(8)	-7(6)
C24'	20(7)	31(7)	48(10)	-5(6)	0(6)	1(5)
C25'	23(6)	29(6)	13(7)	7(5)	1(5)	13(5)
C26'	20(4)	24(4)	20(4)	4(3)	3(3)	1(3)
C27'	13(4)	20(4)	19(4)	-3(3)	2(3)	0(3)
C28'	20(4)	24(4)	25(4)	1(3)	-2(3)	5(3)
C29'	21(7)	34(7)	47(9)	1(6)	3(6)	9(5)
C30'	31(8)	33(7)	93(14)	-8(8)	12(9)	0(6)
C31'	42(9)	31(8)	128(17)	39(9)	34(10)	16(7)
C32'	76(12)	64(10)	64(12)	30(9)	5(9)	5(9)
C33'	33(8)	34(7)	52(10)	7(7)	-12(7)	5(6)

Table 11: Bond Lengths for RR_S_MA_0m (1).

Atom	Atom	Length/Å	Atom	Atom	Length/Å
O1	C26	1.270(11)	O1'	C26'	1.256(11)
O2	C26	1.245(10)	O2'	C26'	1.244(12)
O3	C27	1.418(11)	O3'	C27'	1.411(11)
N1	C18	1.490(11)	N1'	C17'	1.495(11)
N1	C17	1.503(12)	N1'	C18'	1.513(11)
C1	C11	1.529(13)	C1'	C6'	1.502(12)
C1	C6	1.535(12)	C1'	C11'	1.526(12)
C1	C2	1.552(11)	C1'	C2'	1.578(12)

C2	C17	1.532(12)	C2'	C17'	1.536(13)
C2	C3	1.566(13)	C2'	C3'	1.560(12)
C3	C4	1.559(13)	C3'	C4'	1.584(13)
C4	C12	1.491(13)	C4'	C12'	1.503(13)
C4	C5	1.516(13)	C4'	C5'	1.523(13)
C5	C10	1.373(14)	C5'	C10'	1.385(14)
C5	C6	1.386(13)	C5'	C6'	1.387(13)
C6	C7	1.383(13)	C6'	C7'	1.368(13)
C7	C8	1.402(13)	C7'	C8'	1.406(15)
C8	C9	1.402(16)	C8'	C9'	1.382(16)
C9	C10	1.398(16)	C9'	C10'	1.393(15)
C11	C16	1.377(12)	C11'	C16'	1.387(12)
C11	C12	1.395(13)	C11'	C12'	1.395(13)
C12	C13	1.400(14)	C12'	C13'	1.366(13)
C13	C14	1.395(14)	C13'	C14'	1.398(13)
C14	C15	1.362(15)	C14'	C15'	1.396(14)
C15	C16	1.416(15)	C15'	C16'	1.390(13)
C18	C19	1.513(13)	C18'	C20'	1.510(13)
C18	C20	1.526(13)	C18'	C19'	1.547(12)
C20	C21	1.361(12)	C20'	C25'	1.379(13)
C20	C25	1.410(14)	C20'	C21'	1.405(13)
C21	C22	1.396(14)	C21'	C22'	1.398(14)
C22	C23	1.364(17)	C22'	C23'	1.368(15)
C23	C24	1.357(18)	C23'	C24'	1.383(15)
C24	C25	1.430(16)	C24'	C25'	1.411(13)
C26	C27	1.529(12)	C26'	C27'	1.560(13)
C27	C28	1.525(12)	C27'	C28'	1.525(13)
C28	C33	1.373(14)	C28'	C29'	1.354(14)
C28	C29	1.390(13)	C28'	C33'	1.371(15)
C29	C30	1.388(14)	C29'	C30'	1.380(15)
C30	C31	1.386(17)	C30'	C31'	1.386(19)
C31	C32	1.386(17)	C31'	C32'	1.389(19)
C32	C33	1.395(14)	C32'	C33'	1.400(16)

Table 12: Bond Angles for RR_S_MA_0m (1).

Atom	Atom	Atom	Angle/°	Atom	Atom	Atom	Angle/°
C18	N1	C17	116.0(7)	C17'	N1'	C18'	113.4(7)
C11	C1	C6	106.7(8)	C6'	C1'	C11'	110.3(8)
C11	C1	C2	108.4(8)	C6'	C1'	C2'	106.1(7)
C6	C1	C2	104.0(7)	C11'	C1'	C2'	105.4(7)
C17	C2	C1	111.9(7)	C17'	C2'	C3'	109.9(8)
C17	C2	C3	111.6(8)	C17'	C2'	C1'	111.7(7)

C1	C2	C3	109.6(8)	C3'	C2'	C1'	108.0(8)
C4	C3	C2	108.3(8)	C2'	C3'	C4'	109.4(8)
C12	C4	C5	108.9(8)	C12'	C4'	C5'	108.7(8)
C12	C4	C3	104.5(8)	C12'	C4'	C3'	106.3(8)
C5	C4	C3	109.0(9)	C5'	C4'	C3'	106.2(8)
C10	C5	C6	120.5(11)	C10'	C5'	C6'	122.0(10)
C10	C5	C4	127.5(10)	C10'	C5'	C4'	125.0(10)
C6	C5	C4	112.0(9)	C6'	C5'	C4'	113.0(9)
C7	C6	C5	121.2(9)	C7'	C6'	C5'	119.6(10)
C7	C6	C1	124.3(10)	C7'	C6'	C1'	127.2(9)
C5	C6	C1	114.4(9)	C5'	C6'	C1'	113.2(8)
C6	C7	C8	119.8(11)	C6'	C7'	C8'	119.9(10)
C9	C8	C7	117.9(11)	C9'	C8'	C7'	119.5(10)
C10	C9	C8	122.0(10)	C8'	C9'	C10'	121.1(11)
C5	C10	C9	118.6(12)	C5'	C10'	C9'	117.8(11)
C16	C11	C12	122.3(10)	C16'	C11'	C12'	120.5(9)
C16	C11	C1	125.3(10)	C16'	C11'	C1'	126.3(8)
C12	C11	C1	112.3(9)	C12'	C11'	C1'	113.1(8)
C11	C12	C13	119.1(10)	C13'	C12'	C11'	120.1(9)
C11	C12	C4	114.1(9)	C13'	C12'	C4'	127.0(9)
C13	C12	C4	126.7(10)	C11'	C12'	C4'	112.8(9)
C14	C13	C12	118.8(11)	C12'	C13'	C14'	120.3(10)
C15	C14	C13	121.2(12)	C15'	C14'	C13'	119.5(10)
C14	C15	C16	120.9(11)	C16'	C15'	C14'	120.2(9)
C11	C16	C15	117.5(11)	C11'	C16'	C15'	119.4(9)
N1	C17	C2	110.4(8)	N1'	C17'	C2'	112.2(7)
N1	C18	C19	108.1(8)	C20'	C18'	N1'	111.6(8)
N1	C18	C20	110.4(8)	C20'	C18'	C19'	111.3(8)
C19	C18	C20	113.1(8)	N1'	C18'	C19'	107.8(7)
C21	C20	C25	121.3(10)	C25'	C20'	C21'	119.7(9)
C21	C20	C18	121.3(9)	C25'	C20'	C18'	122.7(8)
C25	C20	C18	117.5(9)	C21'	C20'	C18'	117.7(9)
C20	C21	C22	120.8(11)	C22'	C21'	C20'	118.9(10)
C23	C22	C21	119.1(12)	C23'	C22'	C21'	121.8(10)
C24	C23	C22	121.4(13)	C22'	C23'	C24'	119.2(11)
C23	C24	C25	121.2(13)	C23'	C24'	C25'	120.2(10)
C20	C25	C24	116.2(11)	C20'	C25'	C24'	120.1(9)
O2	C26	O1	124.1(9)	O2'	C26'	O1'	126.4(10)
O2	C26	C27	118.3(8)	O2'	C26'	C27'	117.8(9)
O1	C26	C27	117.6(8)	O1'	C26'	C27'	115.7(9)
O3	C27	C28	110.7(8)	O3'	C27'	C28'	111.3(9)
O3	C27	C26	108.9(8)	O3'	C27'	C26'	109.8(8)
C28	C27	C26	112.5(7)	C28'	C27'	C26'	106.6(8)
C33	C28	C29	119.2(9)	C29'	C28'	C33'	120.6(10)

C33	C28	C27	121.2(10)	C29'	C28'	C27'	120.9(10)
C29	C28	C27	119.5(10)	C33'	C28'	C27'	118.3(10)
C30	C29	C28	120.8(11)	C28'	C29'	C30'	121.4(12)
C29	C30	C31	119.8(12)	C29'	C30'	C31'	119.3(12)
C32	C31	C30	119.5(12)	C30'	C31'	C32'	119.4(12)
C31	C32	C33	120.2(13)	C31'	C32'	C33'	120.0(14)
C28	C33	C32	120.4(12)	C28'	C33'	C32'	119.1(12)

Table 13: Torsion Angles for RR_S_MA_0m (1).

A	B	C	D	Angle/°	A	B	C	D	Angle/°
C11	C1	C2	C17	74.2(10)	C6'	C1'	C2'	C17'	179.6(8)
C6	C1	C2	C17	-172.6(9)	C11'	C1'	C2'	C17'	62.6(9)
C11	C1	C2	C3	-50.2(10)	C6'	C1'	C2'	C3'	58.6(9)
C6	C1	C2	C3	63.0(10)	C11'	C1'	C2'	C3'	-58.4(9)
C17	C2	C3	C4	-133.6(8)	C17'	C2'	C3'	C4'	-121.9(8)
C1	C2	C3	C4	-9.1(10)	C1'	C2'	C3'	C4'	0.2(10)
C2	C3	C4	C12	64.4(10)	C2'	C3'	C4'	C12'	58.3(10)
C2	C3	C4	C5	-51.9(10)	C2'	C3'	C4'	C5'	-57.3(10)
C12	C4	C5	C10	128.5(11)	C12'	C4'	C5'	C10'	125.4(11)
C3	C4	C5	C10	-118.1(12)	C3'	C4'	C5'	C10'	-120.5(11)
C12	C4	C5	C6	-53.5(11)	C12'	C4'	C5'	C6'	-55.8(12)
C3	C4	C5	C6	59.9(10)	C3'	C4'	C5'	C6'	58.3(10)
C10	C5	C6	C7	0.8(15)	C10'	C5'	C6'	C7'	-0.3(16)
C4	C5	C6	C7	-177.5(9)	C4'	C5'	C6'	C7'	-179.1(9)
C10	C5	C6	C1	176.8(9)	C10'	C5'	C6'	C1'	-178.4(9)
C4	C5	C6	C1	-1.4(12)	C4'	C5'	C6'	C1'	2.7(12)
C11	C1	C6	C7	-129.5(10)	C11'	C1'	C6'	C7'	-127.7(10)
C2	C1	C6	C7	116.1(10)	C2'	C1'	C6'	C7'	118.6(10)
C11	C1	C6	C5	54.6(10)	C11'	C1'	C6'	C5'	50.4(11)
C2	C1	C6	C5	-59.9(10)	C2'	C1'	C6'	C5'	-63.3(10)
C5	C6	C7	C8	-1.7(14)	C5'	C6'	C7'	C8'	2.0(15)
C1	C6	C7	C8	-177.4(9)	C1'	C6'	C7'	C8'	179.9(10)
C6	C7	C8	C9	1.6(15)	C6'	C7'	C8'	C9'	-2.6(16)
C7	C8	C9	C10	-0.7(17)	C7'	C8'	C9'	C10'	1.4(17)
C6	C5	C10	C9	0.2(16)	C6'	C5'	C10'	C9'	-0.9(16)
C4	C5	C10	C9	178.1(10)	C4'	C5'	C10'	C9'	177.8(10)
C8	C9	C10	C5	-0.2(18)	C8'	C9'	C10'	C5'	0.3(17)
C6	C1	C11	C16	129.9(9)	C6'	C1'	C11'	C16'	133.0(10)
C2	C1	C11	C16	-118.7(10)	C2'	C1'	C11'	C16'	-112.8(10)
C6	C1	C11	C12	-53.4(10)	C6'	C1'	C11'	C12'	-51.2(11)
C2	C1	C11	C12	58.0(10)	C2'	C1'	C11'	C12'	62.9(10)
C16	C11	C12	C13	-2.9(15)	C16'	C11'	C12'	C13'	-1.5(16)

C1	C11	C12	C13	-179.8(8)	C1'	C11'	C12'	C13'	-177.5(9)
C16	C11	C12	C4	176.9(8)	C16'	C11'	C12'	C4'	174.1(9)
C1	C11	C12	C4	0.1(12)	C1'	C11'	C12'	C4'	-2.0(12)
C5	C4	C12	C11	54.7(11)	C5'	C4'	C12'	C13'	-130.1(12)
C3	C4	C12	C11	-61.7(11)	C3'	C4'	C12'	C13'	115.9(11)
C5	C4	C12	C13	-125.4(11)	C5'	C4'	C12'	C11'	54.7(12)
C3	C4	C12	C13	118.2(11)	C3'	C4'	C12'	C11'	-59.3(11)
C11	C12	C13	C14	1.3(14)	C11'	C12'	C13'	C14'	0.5(16)
C4	C12	C13	C14	-178.6(9)	C4'	C12'	C13'	C14'	-174.4(10)
C12	C13	C14	C15	-0.7(16)	C12'	C13'	C14'	C15'	1.3(17)
C13	C14	C15	C16	1.6(16)	C13'	C14'	C15'	C16'	-2.1(16)
C12	C11	C16	C15	3.8(14)	C12'	C11'	C16'	C15'	0.7(15)
C1	C11	C16	C15	-179.8(9)	C1'	C11'	C16'	C15'	176.2(9)
C14	C15	C16	C11	-3.1(15)	C14'	C15'	C16'	C11'	1.1(15)
C18	N1	C17	C2	172.9(7)	C18'	N1'	C17'	C2'	174.9(8)
C1	C2	C17	N1	71.7(10)	C3'	C2'	C17'	N1'	-178.0(8)
C3	C2	C17	N1	-165.0(7)	C1'	C2'	C17'	N1'	62.1(10)
C17	N1	C18	C19	-175.0(8)	C17'	N1'	C18'	C20'	60.2(9)
C17	N1	C18	C20	60.8(10)	C17'	N1'	C18'	C19'	-177.2(8)
N1	C18	C20	C21	58.8(13)	N1'	C18'	C20'	C25'	57.6(12)
C19	C18	C20	C21	-62.4(13)	C19'	C18'	C20'	C25'	-62.9(13)
N1	C18	C20	C25	-121.4(10)	N1'	C18'	C20'	C21'	-123.3(9)
C19	C18	C20	C25	117.3(11)	C19'	C18'	C20'	C21'	116.2(10)
C25	C20	C21	C22	-1.5(17)	C25'	C20'	C21'	C22'	2.1(16)
C18	C20	C21	C22	178.3(10)	C18'	C20'	C21'	C22'	-177.0(10)
C20	C21	C22	C23	-0.2(19)	C20'	C21'	C22'	C23'	-1.9(18)
C21	C22	C23	C24	1(2)	C21'	C22'	C23'	C24'	-1.0(19)
C22	C23	C24	C25	0(2)	C22'	C23'	C24'	C25'	3.6(19)
C21	C20	C25	C24	2.1(16)	C21'	C20'	C25'	C24'	0.4(16)
C18	C20	C25	C24	-177.7(9)	C18'	C20'	C25'	C24'	179.5(10)
C23	C24	C25	C20	-1.1(18)	C23'	C24'	C25'	C20'	-3.3(18)
O2	C26	C27	O3	-157.6(8)	O2'	C26'	C27'	O3'	175.7(8)
O1	C26	C27	O3	22.7(12)	O1'	C26'	C27'	O3'	-6.7(12)
O2	C26	C27	C28	-34.4(13)	O2'	C26'	C27'	C28'	-63.6(12)
O1	C26	C27	C28	145.8(9)	O1'	C26'	C27'	C28'	114.0(9)
O3	C27	C28	C33	32.7(13)	O3'	C27'	C28'	C29'	-156.3(9)
C26	C27	C28	C33	-89.5(12)	C26'	C27'	C28'	C29'	83.9(11)
O3	C27	C28	C29	-149.9(9)	O3'	C27'	C28'	C33'	28.1(13)
C26	C27	C28	C29	87.9(11)	C26'	C27'	C28'	C33'	-91.6(11)
C33	C28	C29	C30	-2.0(15)	C33'	C28'	C29'	C30'	1.3(17)
C27	C28	C29	C30	-179.5(9)	C27'	C28'	C29'	C30'	-174.2(10)
C28	C29	C30	C31	1.6(17)	C28'	C29'	C30'	C31'	2.2(18)
C29	C30	C31	C32	-1.1(17)	C29'	C30'	C31'	C32'	-3(2)
C30	C31	C32	C33	0.9(17)	C30'	C31'	C32'	C33'	1(2)

C29 C28 C33 C32	1.9(15)	C29' C28' C33' C32'	-3.8(17)
C27 C28 C33 C32	179.3(9)	C27' C28' C33' C32'	171.8(10)
C31 C32 C33 C28	-1.4(17)	C31' C32' C33' C28'	2.8(19)

Table 14: Hydrogen Atom Coordinates (Å×10^4) and Isotropic Displacement Parameters (Å^2×10^3) for RR_S_MA_0m (1).

Atom	*x*	*y*	*z*	U(eq)
H3	7457	4922	2482	37
H1C	7425	4270	11197	18
H1D	6353	4577	11950	18
H1A	8242	4897	10077	21
H2	6086	5297	10734	19
H3A	4416	5057	8842	34
H3B	4471	5617	9546	34
H4	5247	5824	7704	31
H7	9492	5777	10591	34
H8	9768	6736	10379	44
H9	8201	7210	9185	51
H10	6435	6748	8184	50
H13	5788	5191	6078	42
H14	6997	4427	5453	47
H15	8499	3956	6630	37
H16	8759	4202	8543	31
H17A	4657	4477	10458	23
H17B	5840	4238	9705	23
H18	5009	3781	11990	22
H19A	7801	3634	12761	45
H19B	6515	3318	13247	45
H19C	6671	3967	13418	45
H21	8211	3408	10787	33
H22	8474	2690	9512	63
H23	6591	2159	8976	67
H24	4459	2339	9623	66
H25	4126	3079	10899	47
H27	7287	5282	4091	22
H29	7065	6088	5244	34
H30	7364	7033	5454	53
H31	7379	7598	3878	64
H32	7187	7205	2103	52
H33	6897	6257	1903	41
H3'	3102	4616	2988	38
H1E	1411	5325	3358	20

H1F	2650	5692	3860	20
H1'1	3092	5258	5427	19
H2'	608	5060	5202	21
H3'1	-745	5312	6555	27
H3'2	-472	5947	6288	27
H4'	309	5752	8232	33
H7'	3638	4343	6375	33
H8'	3332	3744	7889	48
H9'	2004	4021	9354	50
H10'	877	4875	9301	41
H13'	1562	6663	8487	39
H14'	3239	7281	7902	38
H15'	4575	7052	6386	32
H16'	4330	6190	5539	22
H17C	-151	5891	4309	26
H17D	1137	6211	4870	26
H18'	504	6090	2369	20
H19D	3344	5907	1888	44
H19E	2148	6073	996	44
H19F	2154	5477	1556	44
H21'	22	6998	2497	31
H22'	650	7910	2870	46
H23'	2824	8131	3579	50
H24'	4409	7431	3989	39
H25'	3873	6516	3497	26
H27'	2112	4143	1814	21
H29'	1001	3240	1635	41
H30'	206	2443	2454	62
H31'	-264	2445	4354	79
H32'	264	3225	5429	81
H33'	1223	4002	4591	48

Discussion of X-Ray Crystal Stucture of RR-S-MA:

The complex [(*R*,*R*)-**3**•*S*-MA] also crystallized in monoclinic chiral $P2_1$ space group containing two molecules of each components in the asymmetric unit. The crystal structure of [(*R*,*R*)-**3**•*S*-MA] (Figure 34) is isostructural to the [(*R*,*R*)-**3**•*R*-MA] structure. The C–O bond lengths (~1.24-1.26 Å) in the COOH group show that proton transfer has occurred from *S*-MA to amine moiety of the (*R*,*R*)-**3** revealing that the complex is salt. The neighboring symmetry independent *S*-MA molecules generate the helical chain similar to [(*R*,*R*)-**3**•*R*-MA] through O-

H···O hydrogen bond (H···O = 1.907 Å, O…O = 2.720 Å /O-H···O = 163° and H···O = 1.598 Å, O···O = 2.827 Å /O-H···O = 155°) involving hydroxyl H-atom and carbonyl oxygen of the carboxylic group having graph set notation $C_2^2(10)$, wherein C(10) denotes a chain motif with ten atoms in the repeat unit. Both symmetry independent (*R*,*R*)-**3** molecules are associated with this extended chain on either side through N-H···O hydrogen bonding interactions to generate the layered structure. One of the N-H proton of (*R*,*R*)-**3** is involved in the bifurcated N-H···O hydrogen bonding interactions with the carbonyl (H···O = 1.925 Å, N···O = 2.739 Å /O-H···O = 138°; H…O = 1.901 Å, N···O = 2.729 Å /O-H···O = 137°) and hydroxyl (H···O = 2.013 Å, N···O = 2.818 Å /O-H···O = 138°; H···O = 2.059 Å, N···O = 2.878 Å /O-H···O = 139°) oxygens of *S*-MA molecules with graph set notation $[R_1^2(5)]$ representing hydrogen bonding ring motif consisting of five atoms, with one donor group and two acceptor groups. The other N-H proton forms a N-H···O hydrogen bonding interactions with the carboxyl oxygen of *S*-MA (H···O = 1.821 Å, N···O = 2.788 Å /O-H···O = 165°; H···O = 1.959 Å, N···O = 2.916 Å /O-H···O = 162°) with graph set notation [D(2)] representing hydrogen bonding finite motif consisting of two atoms. Similar to the crystal structure of [(*R*,*R*)-**3**•*R*-MA], two molecules of each *S*-MA and (*R*,*R*)-**3** constitute a tetrameric structure through hydrogen bonding interactions which is extended along the *a*-axis to generate the chain structure. The neighboring chains are loosely connected to each other roughly along the *b*-axis *via* hydrophobic interactions. To the best of our knowledge there are very few reports on the crystal study of the structure of the salt of test substrate and the CSA to understand the supramolecular interactions. The experimental observations of shielding and deshielding effects in the two pairs in ^{1}H NMR analysis corroborated well with the information obtained from these crystal structures, even though one needs to be cautious to compare the two.

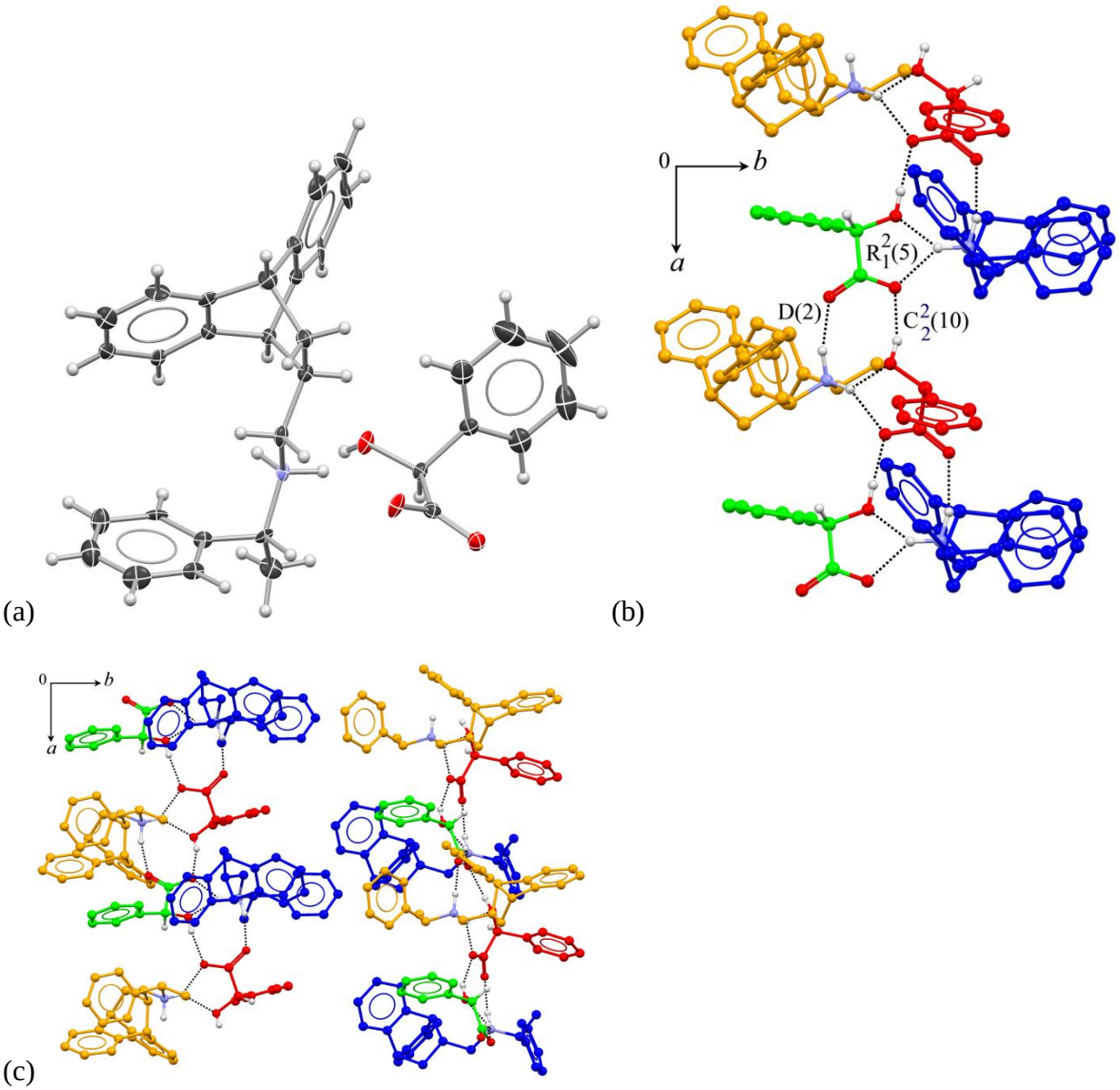

Figure 34 (a) ORTEP view of (*R*,*R*)-**3**•*S*-MA salt. The displacement ellipsoids are drawn at 40% probability level and H atoms are shown as small spheres of arbitrary radii. (b) Association of the symmetry independent (*R*,*R*)-**3** molecules to the O-H···O hydrogen bonded helical chain of *S*-MA (green and red) through N-H···O hydrogen bonding interactions generating an extended chain assembly. (c) linking of the neighboring helical chains through van der Waals forces.